General Disclaimer

One or more of the Following Statements may affect this Document

- This document has been reproduced from the best copy furnished by the organizational source. It is being released in the interest of making available as much information as possible.

- This document may contain data, which exceeds the sheet parameters. It was furnished in this condition by the organizational source and is the best copy available.

- This document may contain tone-on-tone or color graphs, charts and/or pictures, which have been reproduced in black and white.

- This document is paginated as submitted by the original source.

- Portions of this document are not fully legible due to the historical nature of some of the material. However, it is the best reproduction available from the original submission.

metrology research, inc.

Final Report

CLOUD COVER EFFECTS ON SIGNAL ATTENUATION AT DSN SITES

by

T. B. Smith
C.-W. Chien

Submitted to

Jet Propulsion Laboratory
Pasadena, California

Subcontract No. 952757
Under NASA Contract NAS7-100
(Task Order No. RD-20)

by

Meteorology Research, Inc.
464 West Woodbury Road
Altadena, California 91001

24 April 1970

MRI70 FR-922

ABSTRACT

A computational system has been established for the calculation of attenuation statistics at 2.3 G Hz and 8.5 G Hz at each of three DSN sites: Goldstone, Madrid, and Canberra. Data are presented in terms of frequency of occurrence of various attenuation values for each of four seasons and each of four times of day.

Results indicate that, statistically, calculated values are lowest at Goldstone and highest at Madrid. Winter months generally show larger attenuation values with minima occurring during summer. Lowest values characteristically occur during the night and highest values in the afternoon although nocturnal low clouds at Canberra yield relatively high attenuation values more frequently than appears in nighttime conditions at the other two sites.

Possible errors in the calculation have been examined and found to result mainly from lack of adequate observational data. Cloud characteristics in terms of ice or water and in terms of drop size (mean and concentration) are the two factors primarily responsible for the possible errors.

This work was performed for the Jet Propulsion Laboratory, California Institute of Technology, sponsored by the National Aeronautics and Space Administration under Contract NAS7-100.

TABLE OF CONTENTS

I. INTRODUCTION

Degradation of telemetry signals from outside the earth's atmosphere occurs as a result of passage through cloud systems. Scattering by the cloud particles increases the inherent noise in the transmitted signals while the total number and amount of scattering particles causes signal attenuation.

Analytic expressions are available for the computation of the attenuation effects as a function of radiation wavelength. Input parameters required for the computations are the concentration and size distribution of the scattering particles, their ice vs. water characteristics, and the temperatures and depth of the layer containing the particles.

Observations of these cloud parameters are not made on a routine basis. Observations, generally reported, are extent of cloud cover (in categories of clear, scattered, broken, or overcast) and heights of cloud base. Depths of clouds are reported only occasionally by aircraft, and information on base and top heights of high clouds (above 20,000 feet) is usually not reported at all.

Information on number concentration and drop size is available only from research flights made usually for the purpose of studying the evolution of precipitation in various cloud types. Meaningful average values of the required cloud parameters can be established from this information to cover the various cloud types which may be encountered.

An attempt has been made in the following report to obtain attenuation statistics for three DSN sites: Goldstone, Madrid, and Canberra. Typical values of cloud parameters were assigned for each cloud type. Frequencies of occurrence for each cloud type at each site were obtained from available climatological data. Since the input parameters had to be estimated from data sources not specifically intended to be used for this purpose, estimates of the possible errors in the statistics are included.

II. ATTENUATION BACKGROUND

The attenuation of electromagnetic waves by hydrometeors in the atmosphere may result from both absorption and scattering depending on the size of the particles and whether they are composed of water or ice. A complete theory for spherical particles of any material in a non-absorbing mechanism was developed by Mie (1908). Mie's work has been restated by Straton (1941), Goldstein (1946), and by Kerr (1951). From the Mie theory, it is possible to derive equations for Q_s the scattering cross section, Q_a the absorption cross section, and Q_t the total attenuation cross section.

Two frequencies (2.3 and 8.5 G Hz) are of interest in the present study. These frequencies are similar to those used in meteorological radar systems, and the effects of cloud particles on signal attenuation have been studied rather extensively.

The following discussion has been collected from the literature of radar meteorology and cloud physics. In particular, the books of Mason (1957), Battan (1959), Fletcher (1962), and Bean and Dutton (1966), and review papers of Gunn and East (1954) and Atlas (1964) are the basis for this summary.

The cross sections for a spherical particle are

$$Q_s = \frac{\lambda^2}{2\pi} \sum_{n=1}^{\infty} (2n + 1) \left(|a_n|^2 + |b_n|^2\right)$$

$$Q_a = \frac{\lambda^2}{2\pi} \left(- R_e\right) \sum_{n=1}^{\infty} (2n + 1) \left(a_1 + b_n\right)$$

and $$Q_t = Q_s + Q_a$$

where λ = wavelength

a_n = coefficient of nth magnetic mode

b_n = coefficient of nth electric mode

The coefficients a_n and b_n are made up of spherical Bessel functions of order n. The arguments of these functions are m, the complex index of refraction and α, a non-dimensional size parameter. α is defined as the ratio $2\pi r/\lambda$ where r is the radius of the particle.

For particles that are small ($\alpha << 1$), the Rayleigh approximations are applicable.

$$Q_s = \frac{128}{3} \frac{\pi^5 r^6}{\lambda^4} \left| \frac{m^2 - 1}{m^2 + 2} \right|^2$$

$$Q_a = \frac{8\pi^2 r^3}{\lambda} \mathrm{Im} \left(- \frac{m^2 - 1}{m^2 + 2} \right)$$

For large particles, the exact Mie equations must be used.

Figure 1 shows curves of $Q_t/\pi r^2$ for water at 0°C for a wavelength of 3.2 cm as computed by Herman et al. (1961). As α increases beyond a value of 2, $Q_t/\pi r^2$ rapidly approaches an asymptote of 2. For ice, Herman and Battan (1961) have computed $Q_t/\pi r^2$ versus α as shown in Fig. 2. The value of Q_t oscillates more violently than that of water. Since the attenuation by ice particles is due almost entirely to scattering and not to absorption, the erratic nature of Q_t curve for ice is due to the interference effects between the front and back surfaces of ice spheres. Nevertheless, $Q_t/\pi r^2$ for ice eventually approaches an asymptote of 2 as in the case of water. For small particles, the attenuation by ice is negligible with respect to that of water. However, attenuation by large ice spheres is comparable to that of water and sometimes exceeds it.

For particles of non-spherical shape, the scattering a attenuation properties are more complex. Figure 3 after Atlas et al. (1953) for small particles, illustrates the attenuation for randomly oriented spheroids, either oblate or prolate, relative to those corresponding to equivolume spheres. Ice, because of its small refractive index, shows small shape effects even when the particles are highly distorted. The effects are greatly magnified in the case of water. However, water drops do not take on extreme shapes. These results are pertinent to water-coated non-spherical ice particles and to non-spherical hail coated by a shell of spongy ice. These randomly oriented particles always scatter more intensely than would spheres of equal volume. When the particles are preferentially oriented, so that the major axes are parallel to the direction of polarization of the incident field, the scattered radiation intensity is greater than would occur from randomly oriented particles. When minor axes of the particles are parallel to the direction of polarization. the scatter radiation intensity is less than that from spheres of equal volume.

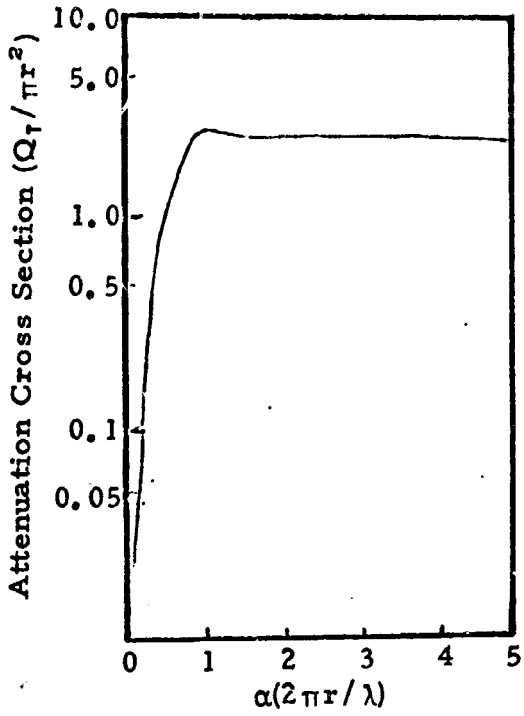

Fig. 1. ATTENUATION CROSS SECTION FOR WATER SPHERES AT 0°C AND 3.2 cm (after Herman et al., 1961)

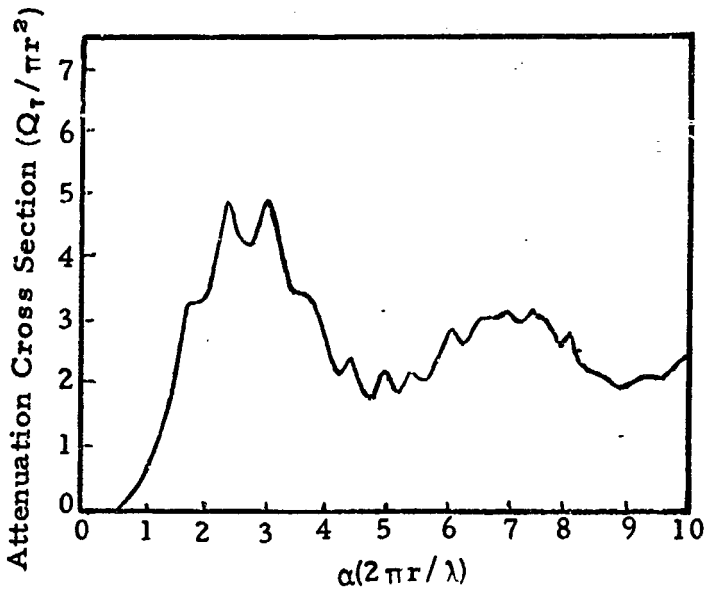

Fig. 2. ATTENUATION CROSS SECTION FOR ICE SPHERES (after Herman and Battan, 1961)

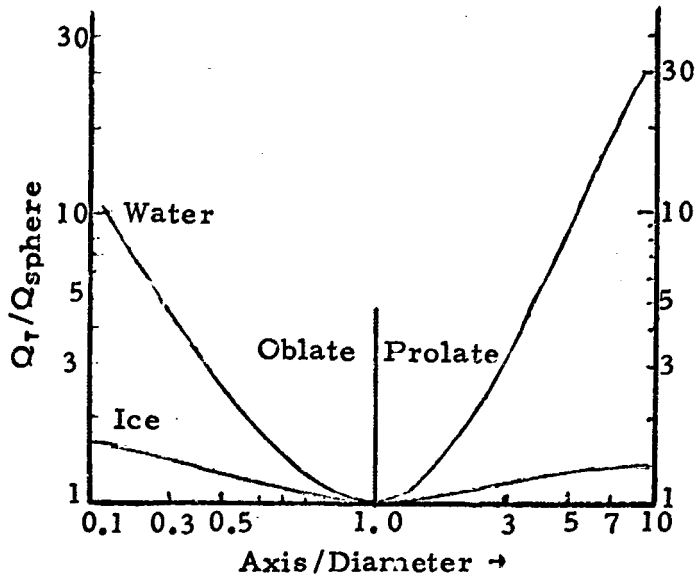

Fig. 3. ATTENUATION DEPENDENCE ON SHAPE FOR ICE AND WATER (after Atlas et al., 1953)

Battan and Herman (1962) calculated the normalized attenuation cross section for spheres of a homogeneous mixture of ice and water. As the percentage of water is increased, the cross sections of spheres of diameter greater than 3 cm decrease fairly rapidly and the amplitude of oscillations diminishes.

The cloud systems are composed of ice or water particles or combinations of ice and water. Amount of hydrometeor content in any given cloud depth may vary considerably from one cloud to another. Cloud depths, in turn, will also vary. Internally, the size distributions of the cloud particles are heterogeneous, ranging from a few microns diameters to several millimeters in the case of precipitation particles. Shapes of cloud droplets may be assumed to be spherical except for the larger raindrops, but many ice particles tend to be quite irregular in shape. Thus, the size, number, and shapes of the scattering particles can vary widely depending on cloud type and stage of cloud development.

So far, only the scattering and attenuation cross section of individual particles as a function of size, shape, orientation, and phase have been considered. The total attenuation cross section of a volume of particles is the summation over a unit volume which includes the particle size-distribution in addition to the characteristics of these particles.

Much effort has been devoted to determine the size distribution of cloud particles. The general characteristics of cloud drop spectra are shown in Table I. Clouds which are not likely to precipitate consist of relatively large numbers of small droplets. Thicker denser clouds contain considerably larger droplets. Low stratus and fog generally consist of rather low concentrations of relatively large droplets.

Generally, it is more practical to estimate the liquid water content than the drop size distribution. Reliable measurements of both parameters are scarce, but one can make reasonable estimates of liquid water content from the vertical extent of the cloud and temperature of its base. Liquid water content and drop number concentrations yield drop size data.

The size distribution of raindrops might be expected to vary considerably with the character of rain, with the type of cloud from which they fall, and also with rainfall intensity. Furthermore, the drop-size distribution may change with time. There is good reason to believe that the drop size spectrum must change continually as the rain falls toward the ground because of coalescence between drops, the separating effects of wind shear, and gravitational settling and evaporation in the sub-cloud layer. Very little information is known about the concentration and size distribution of raindrop variations in space, height, and time during a storm.

Table I

CHARACTERISTICS OF CLOUD DROP DISTRIBUTIONS
(after Mason, 1957)

Cloud Type	Concentration	Mean Radius	Size Range
Fair Weather Cumulus	300/cm^3	9 μm	3-33 μm
Cumulus Congestus	64	24	3-83
Cumulonimbus	72	20	2-100
Stratocumulus	350	4	1-12
Altostratus	450	5	1-13
Nimbostratus	330	6	1-20
Stratus	260	6	1-22

Several versions of empirical curve fitting have been made to the raindrop size distribution. Most notable are that of Laws and Parson (1943), Marshall and Palmer (1948), Best (1950), Blanchard (1953), and many others. In practice, rain attenuation has been expressed as a function of precipitation rate, which depends on both the liquid water content and the fall velocity of the drops involved. The latter quantity depends on the size of the drops. The higher the rainfall rate, the larger the drops and also the greater range in size of drops.

Little is known about the attenuation of snow. When the snow is dry, the attenuation is substantially smaller than with rain of equal liquid water content. However, with melting snow or ice particles, the attenuation can be quite large. With melting non-spherical particles, the attenuation would be greater than with rain of equal mass.

The greatest uncertainty in predictions of attenuation is the extremely limited knowledge of size distribution, concentration, and particle characteristics. All these parameters will vary under different climatic and weather conditions. There is very little evidence that one can assign some unique values for certain known cloud or rain types. However, for many practical purposes, certain averages over time or space may be adequate. Figures 4 and 5, respectively, show such attempts at the estimation of the attenuation by cloud and rainfall (Haroules and Brown, 1969).

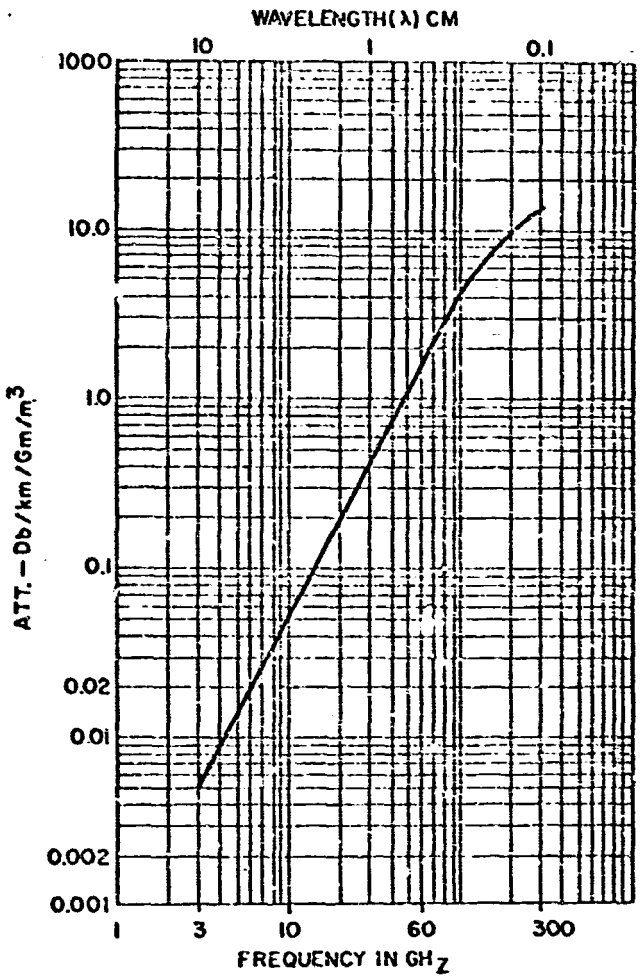

Fig. 4. CLOUD OR FOG ATTENUATION
(after Haroules and Brown, 1969)

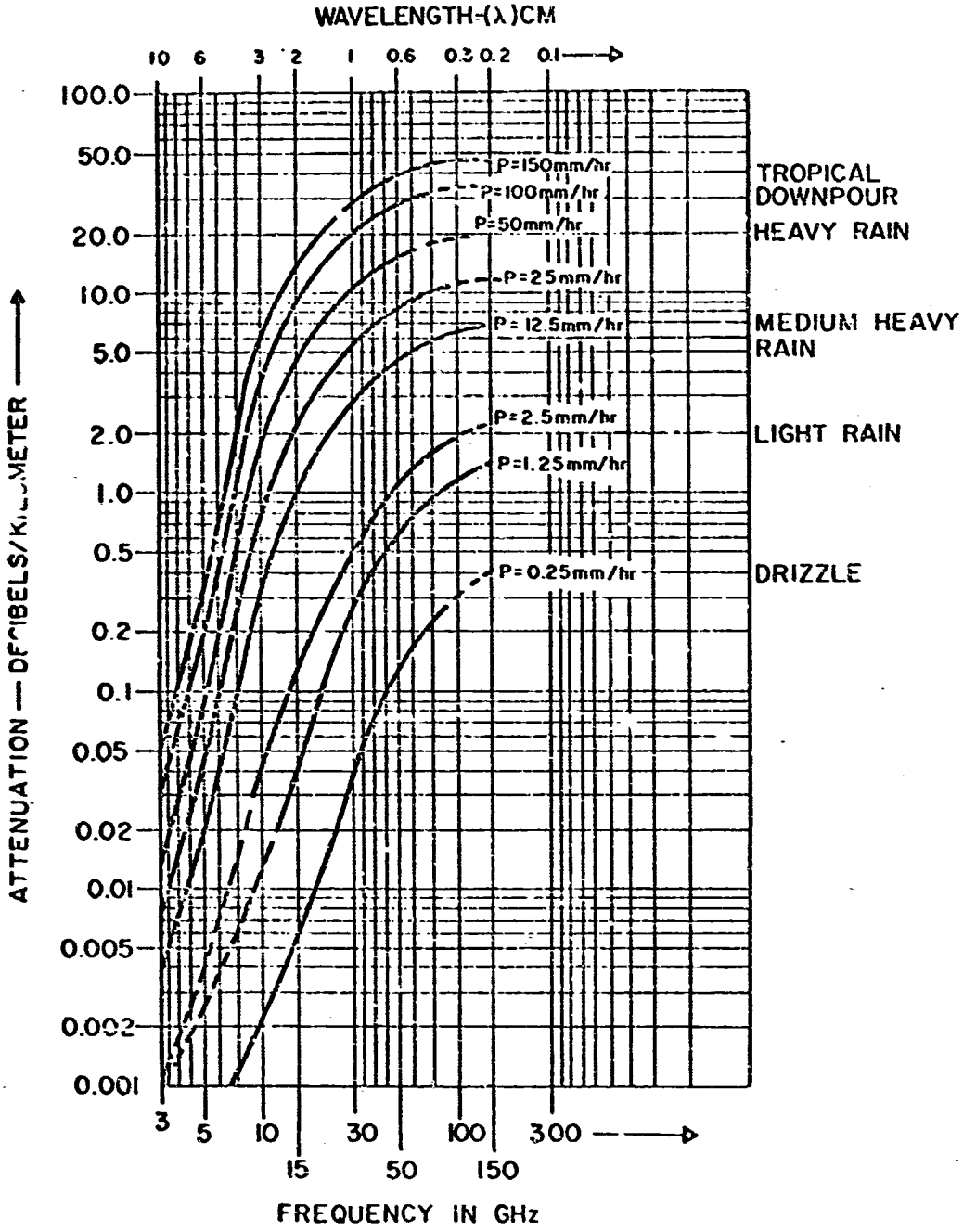

Fig. 5. RAINFALL ATTENUATION
(after Haroules and Brown, 1969)

III. ATTENUATION CALCULATIONS

Attenuation due to cloud systems was calculated in a manner similar to that used by Dutton (1968) but with somewhat different inputs from the meteorological standpoint. The general meteorological practice of cloud reporting (high, middle, and low clouds) was followed in order to adapt standard weather observations to the calculation procedure. Each cloud observation was assigned an average temperature, cloud depth, and cloud coverage, based on available data and reasonable estimates of the data such as cloud depth which is not usually observed. The cloud drop characteristics were selected from the basic data in Table I as follows:

Table II

ASSUMED DROP SIZE CHARACTERISTICS

	Low Clouds	Middle Clouds	High Clouds
Winter and Fall			
Mean radius	7 μm	6 μm	40 μm
Number/cm^3	300	300	1
Summer and Spring			
Mean radius	9	6	40
Number/cm^3	300	300	1

The scattering and absorption coefficients were calculated for each cloud from the following equations:

$$Q_s = \frac{128\,\pi_i^5}{3\lambda^4}\left|\frac{m^2-1}{m^2+2}\right|^2 10^{-24}\int_0^\infty r^6\,n(r)dr\cdots(cm^{-1})$$

$$Q_a = \frac{8\pi^2}{\lambda}\,Im\left(-\frac{m^2-1}{m^2+2}\right)10^{-12}\int_0^\infty r^3 n(r)dr\cdots(cm^{-1})$$

The values of Q_a are larger than Q_s for all conditions considered in the present study.

The total attenuation is then evaluated from:

$$A(db) = 4.343\sum_{i=1}^{3}(Q_s + Q_a)_i\,D_iC_i$$

where D_i is the depth of cloud (in cm), and C_i is the percent of sky covered by the cloud system. The calculated values apply to a zenith-

pointing ray direction and the attenuation values should be increased for off-zenith directions by $1/\cos \beta$ where β is the angle from the zenith.

Cloud cover data for Goldstone were obtained by examining observational records from Daggett, California, at four-hourly intervals for a period of one year. Each observation was assigned a cloud type and depth. Average temperature data were determined from radiosonde observations made at Edwards AFB. Cloud cover data were summarized for the year and compared to long-term averages at Edwards to assure that the single year of record at Daggett was not abnormal. Each four-hourly data set was used to generate an attenuation value, and the cumulative frequencies of these values are presented in the following section.

In the case of Madrid, day-to-day cloud cover data were not available and reliance was placed on long-term statistics of cloud cover frequencies by seasons. Daily radiosonde data from Madrid proved to be highly useful in determining depths of cloud formations, and the cloud cover statistics served to identify cloud type and percent of sky covered with clouds. Numbers of days per season with various cloud characteristics were generated from this information and formed the basis for the attenuation frequency results.

At Canberra, the only suitable data on cloud characteristics came from long-term statistics on cloud cover frequencies by seasons. These summaries listed frequency of cloud cover of varying amounts for low clouds and for total cloud cover. Temperature data were not available on a daily basis but were obtained from seasonal average data. Thirteen classes of "cloud days" were established for each season including various combinations of low, middle, and high clouds. Frequencies of occurrence of each of these "cloud day" types were determined in a manner which would best conform to the long-term average cloud statistics which were available. These data were then used to compute the attenuation statistics.

IV. ATTENUATION STATISTICS

Values of attenuation have been calculated as indicated in the previous section for Goldstone, Madrid, and Canberra. The data have been grouped into four seasons (December-February, March-May, June-August, and September-November) and into four time periods during the day (0000, 0600, 1200, and 1800 local standard time). Cloud cover summaries were not available at Canberra for the time period of 0000 local time and this period is not included in the graphs which follow.

Attenuation data have been plotted in the form of cumulative frequencies of occurrence starting from the highest calculated values. Clear days make up the difference between the largest values shown and 100 percent for each case.

Table III

ATTENUATION GRAPHS

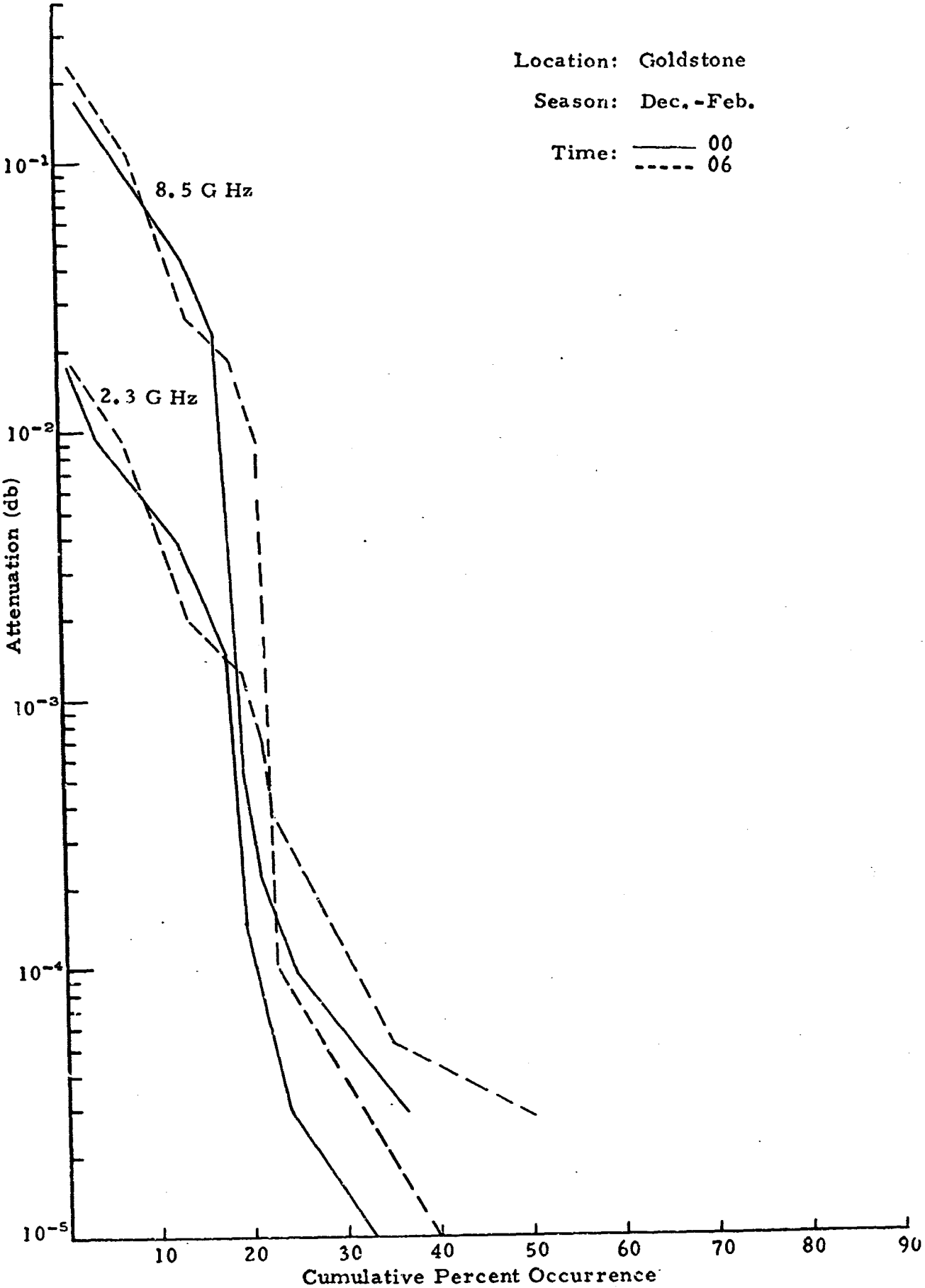

Fig. 6. ATTENUATION FACTORS

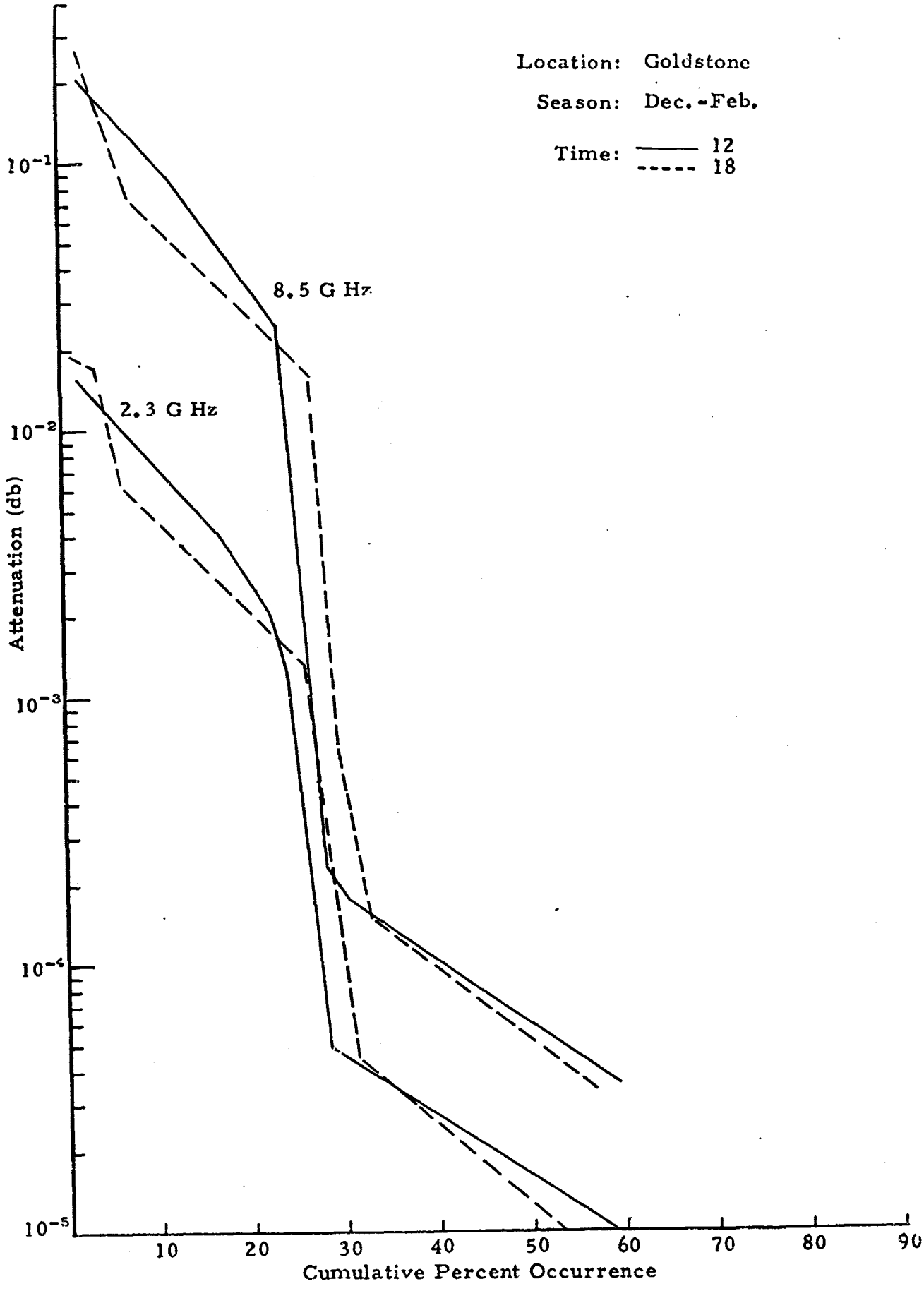

Fig. 7. ATTENUATION FACTORS

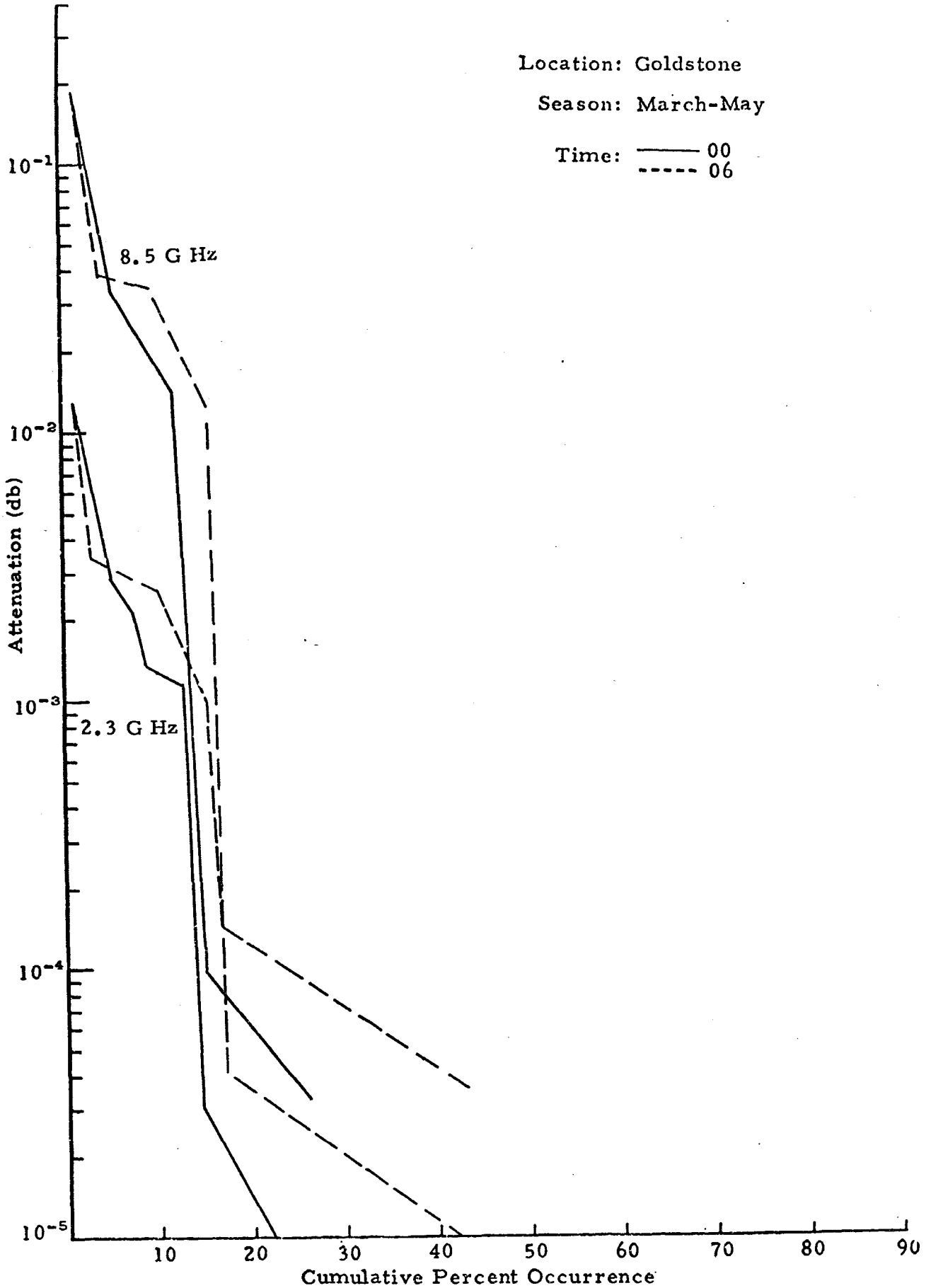

Fig. 8. ATTENUATION FACTORS

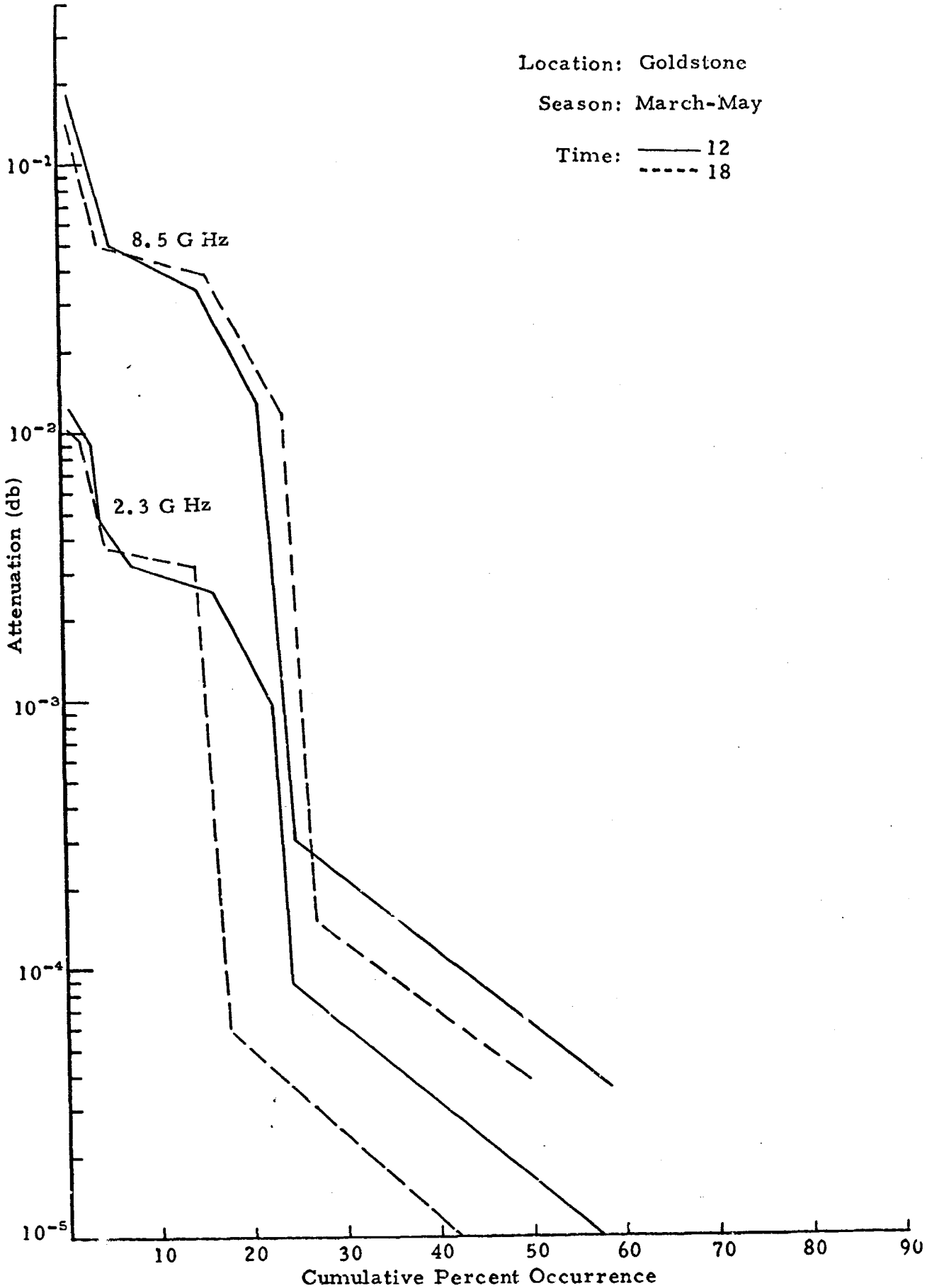

Fig. 9. ATTENUATION FACTORS

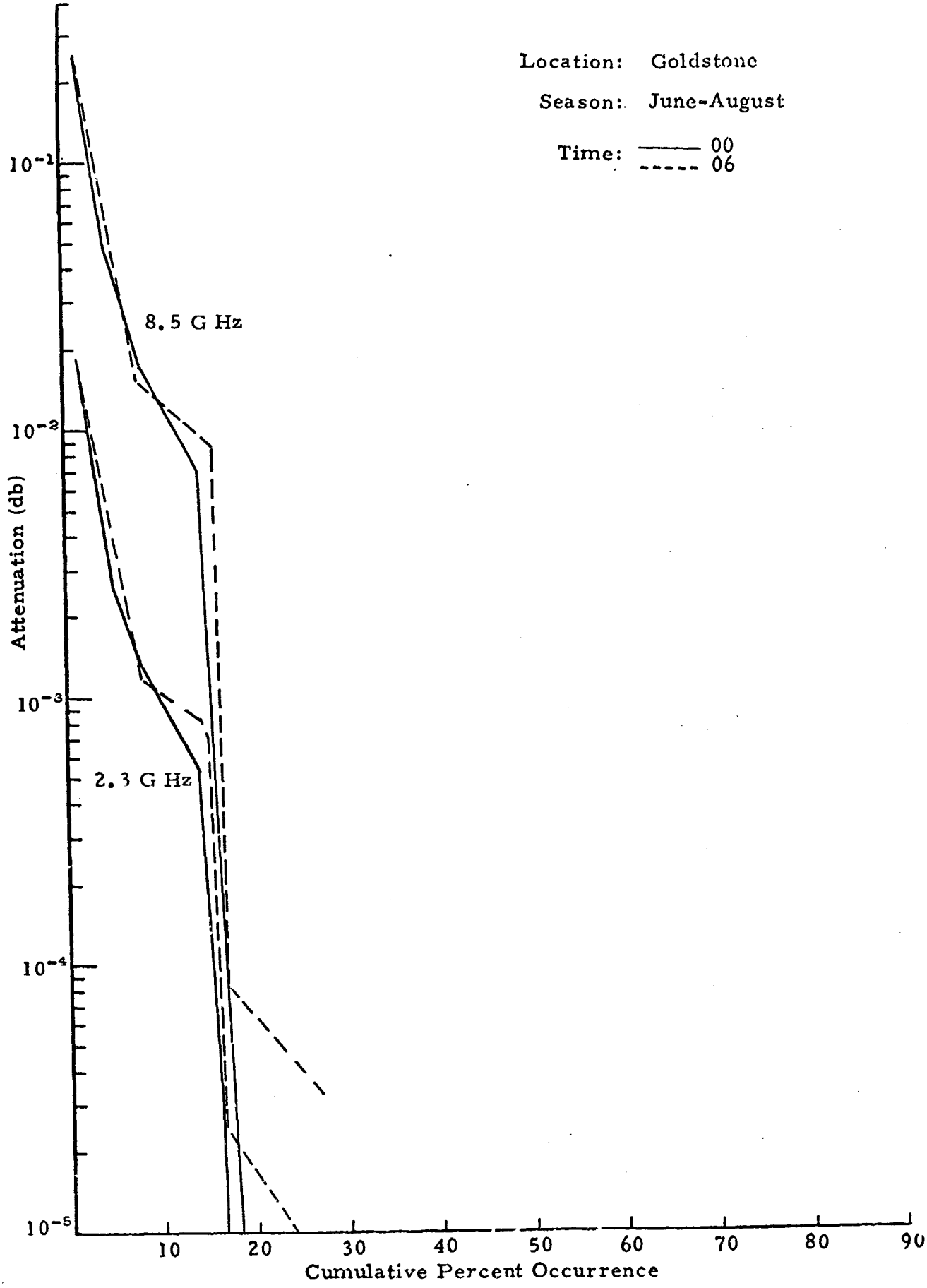

Fig. 10. ATTENUATION FACTORS

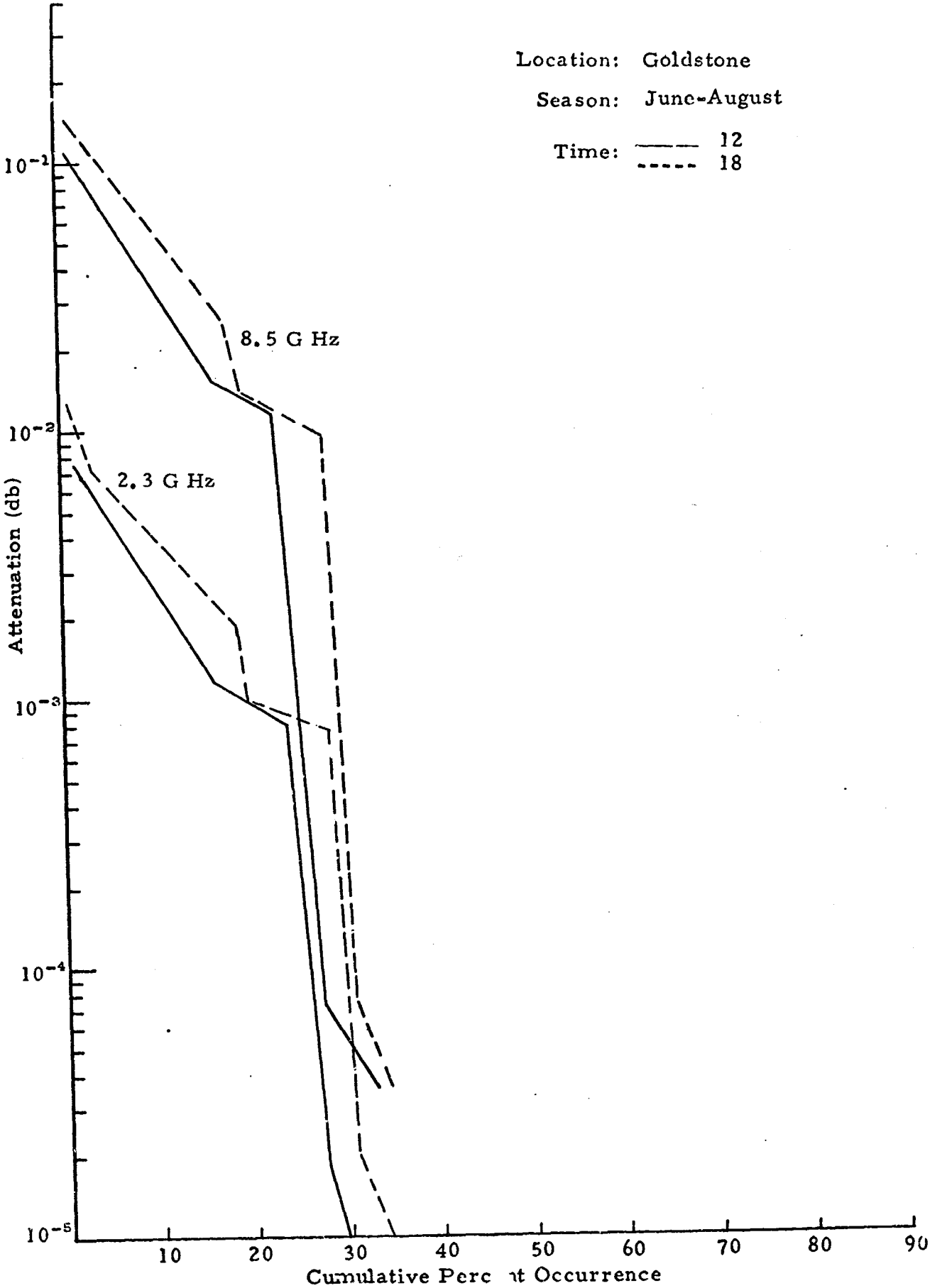

Fig. 11. ATTENUATION FACTORS

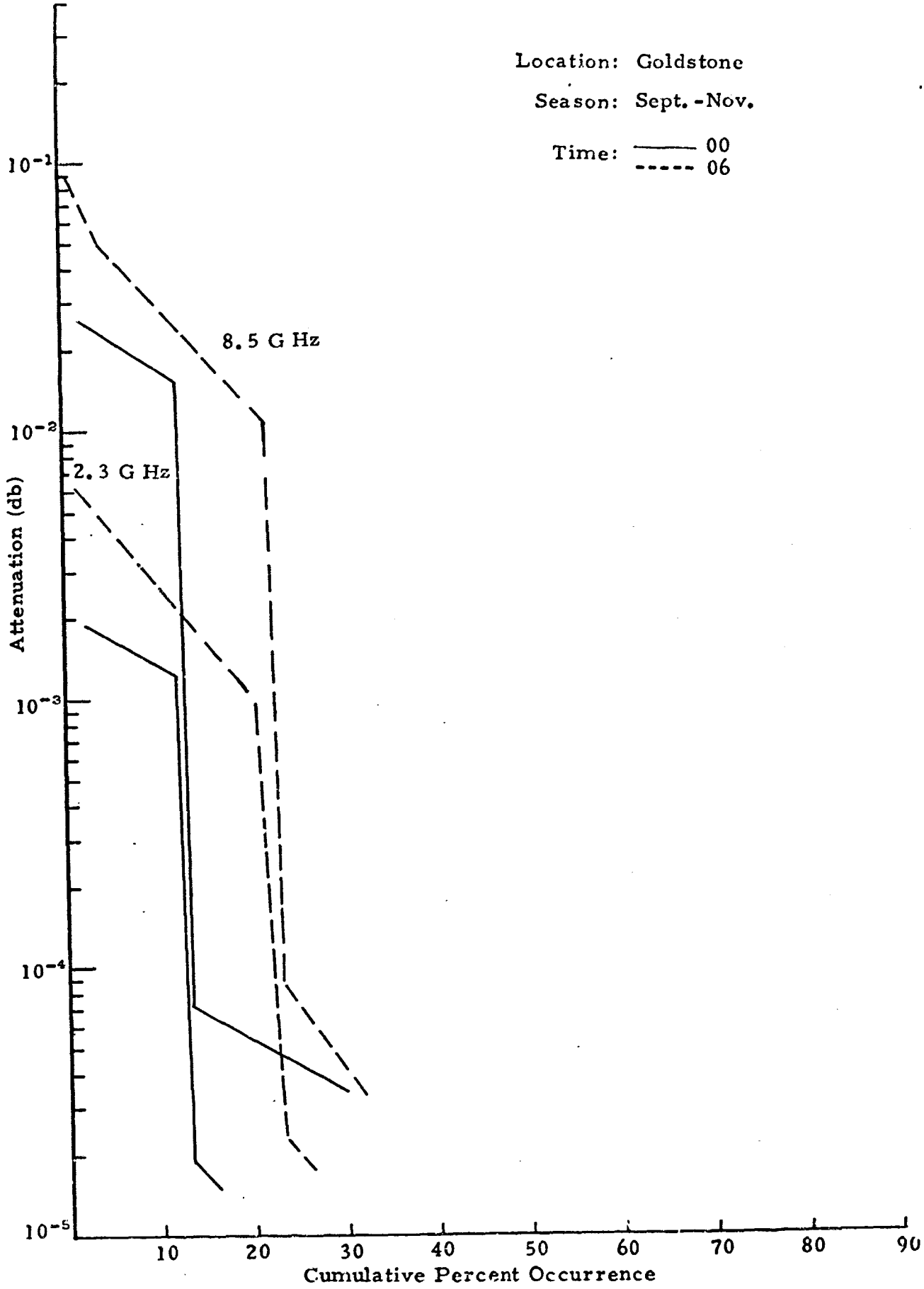

Fig. 12. ATTENUATION FACTORS

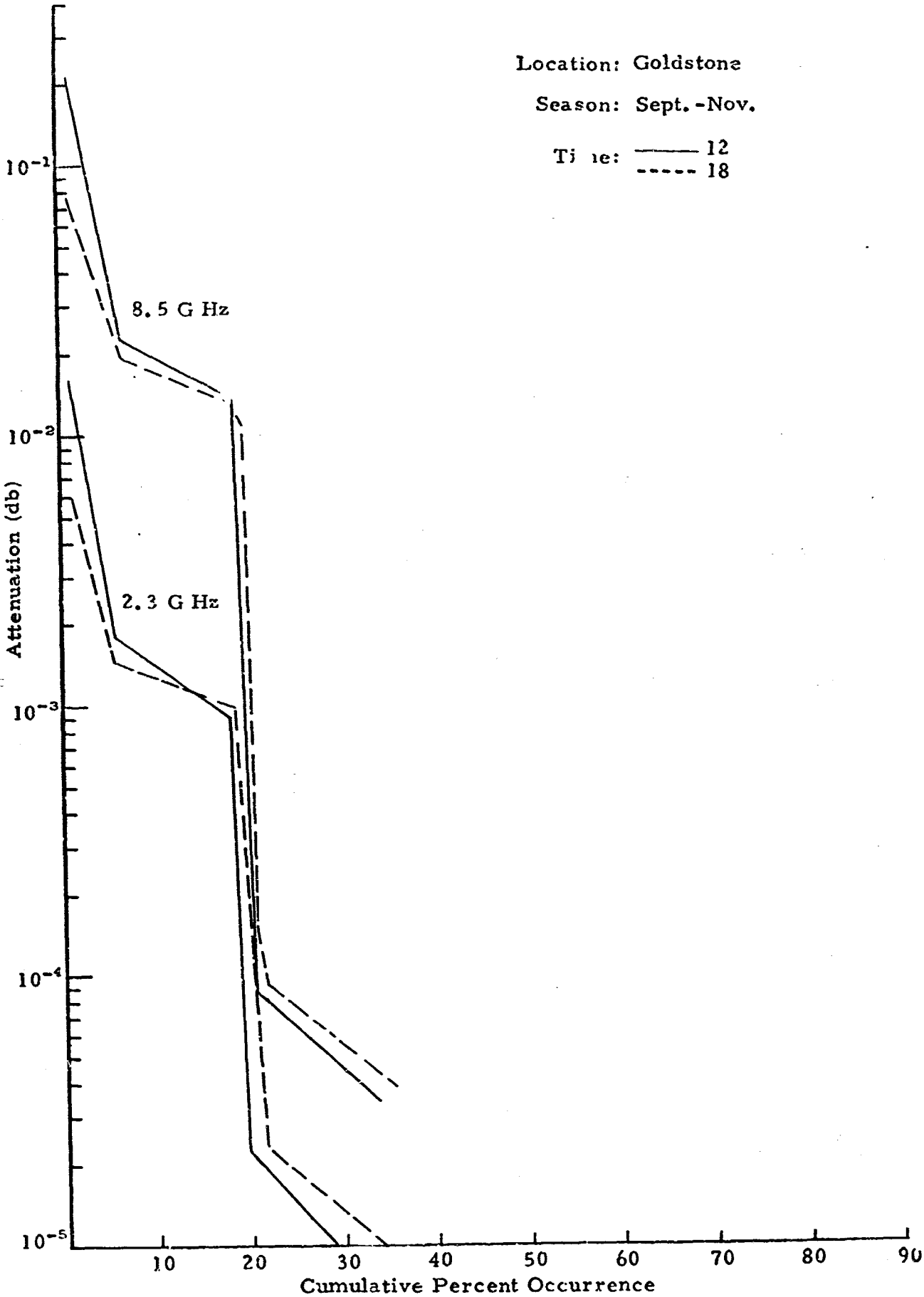

Fig. 13. ATTENUATION FACTORS

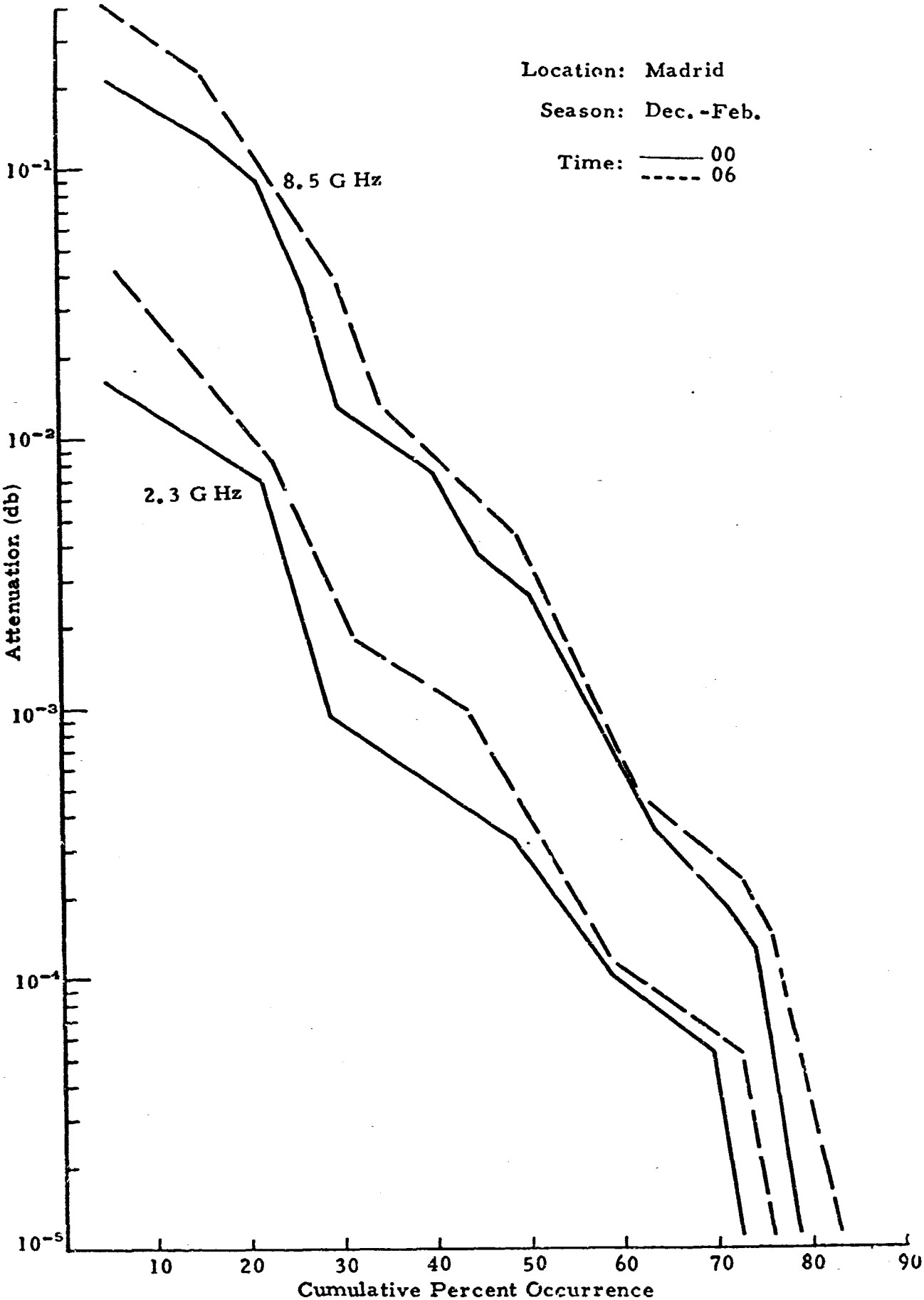

Fig. 14. ATTENUATION FACTORS

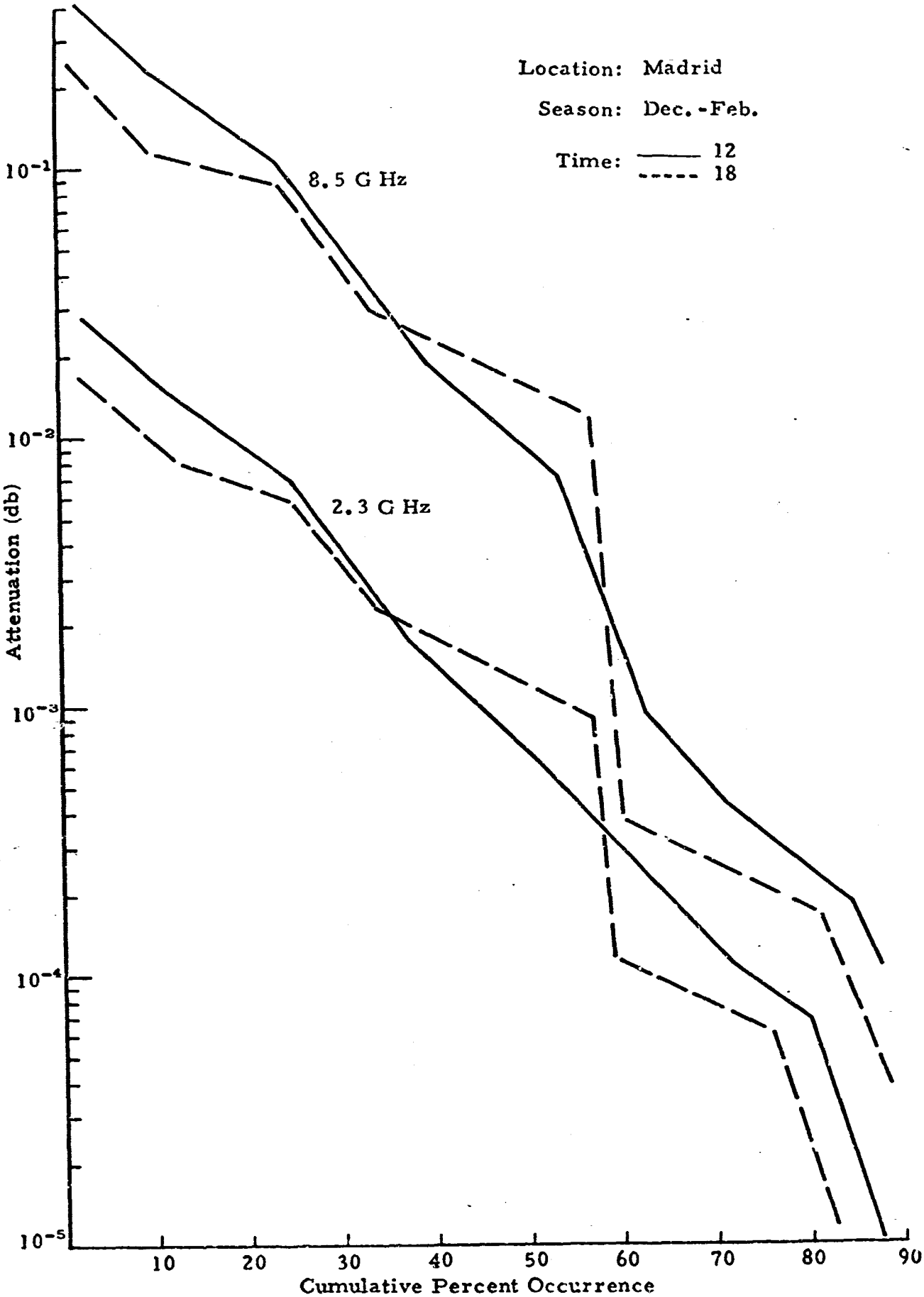

Fig. 15. ATTENUATION FACTORS

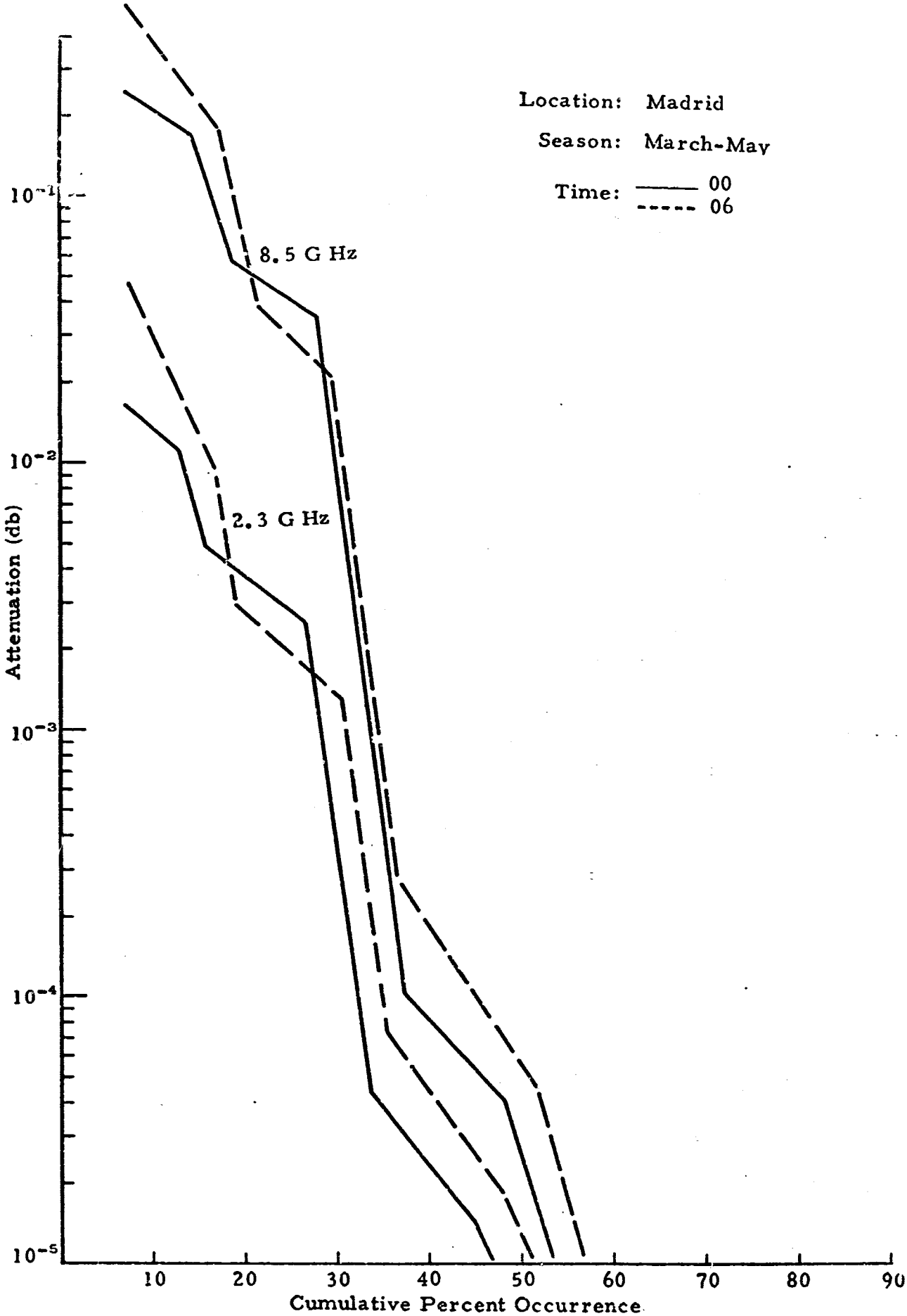

Fig. 16. ATTENUATION FACTORS

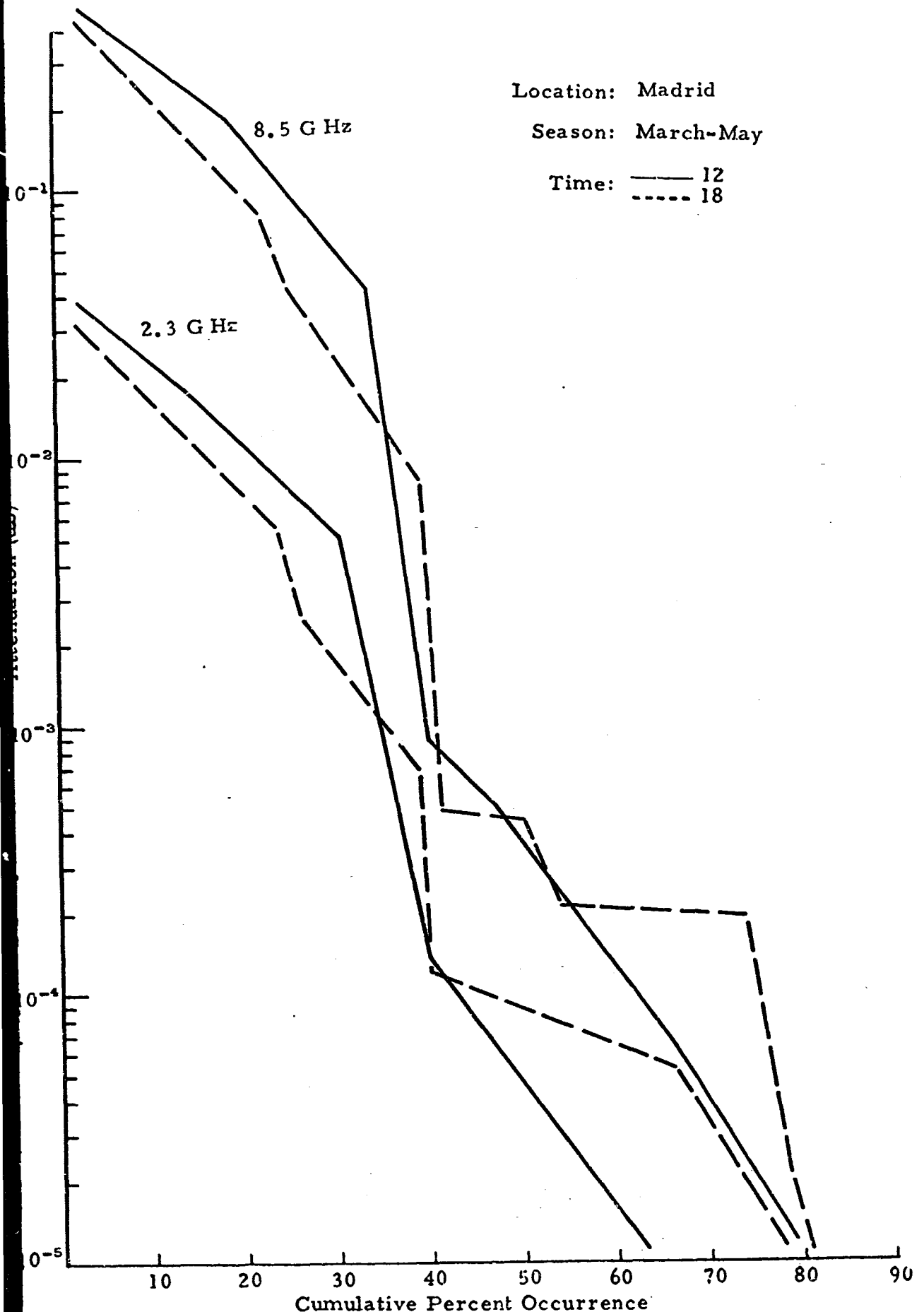

Fig. 17. ATTENUATION FACTORS

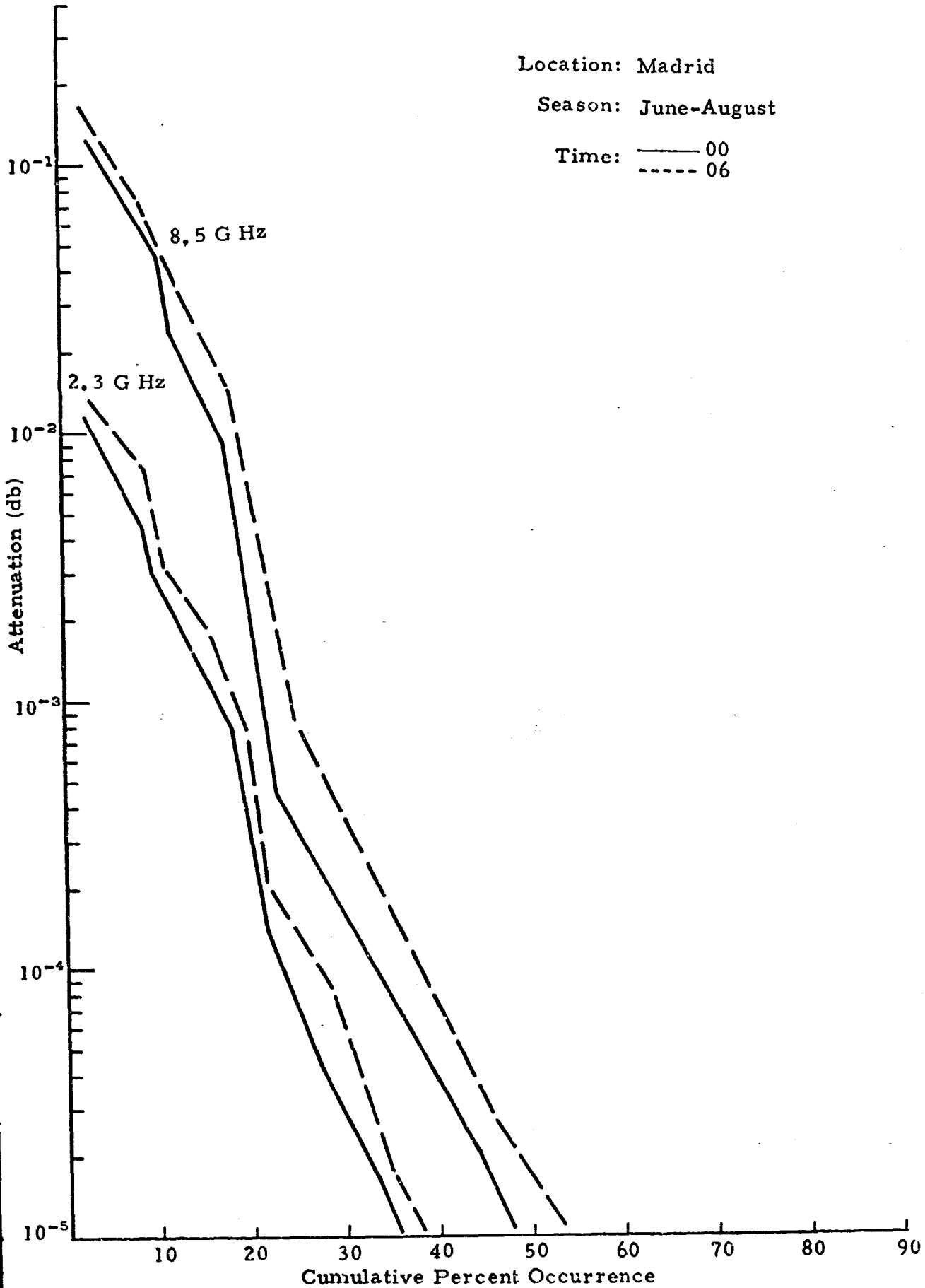

Fig. 18. ATTENUATION FACTORS

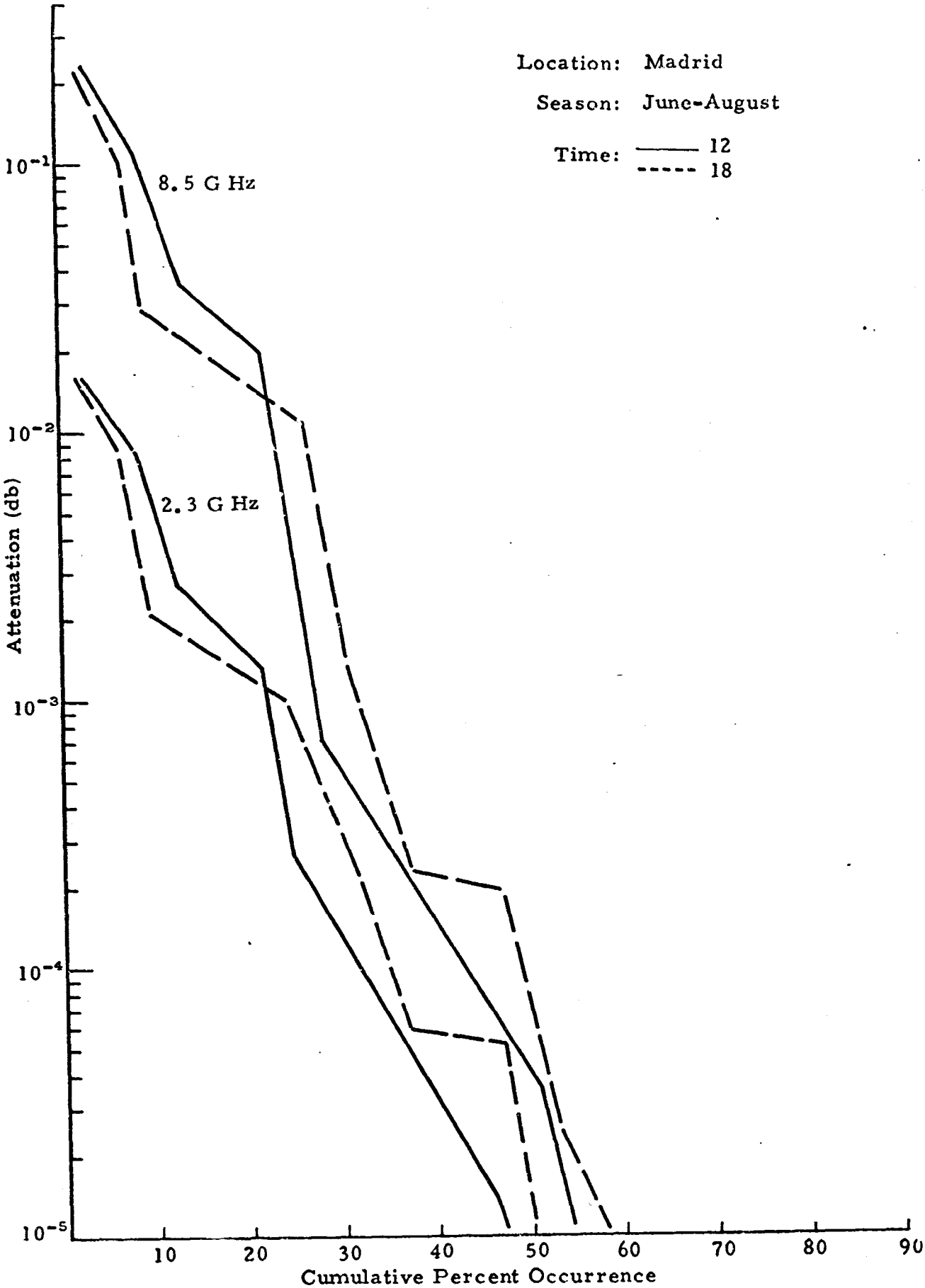

Fig. 19. ATTENUATION FACTORS

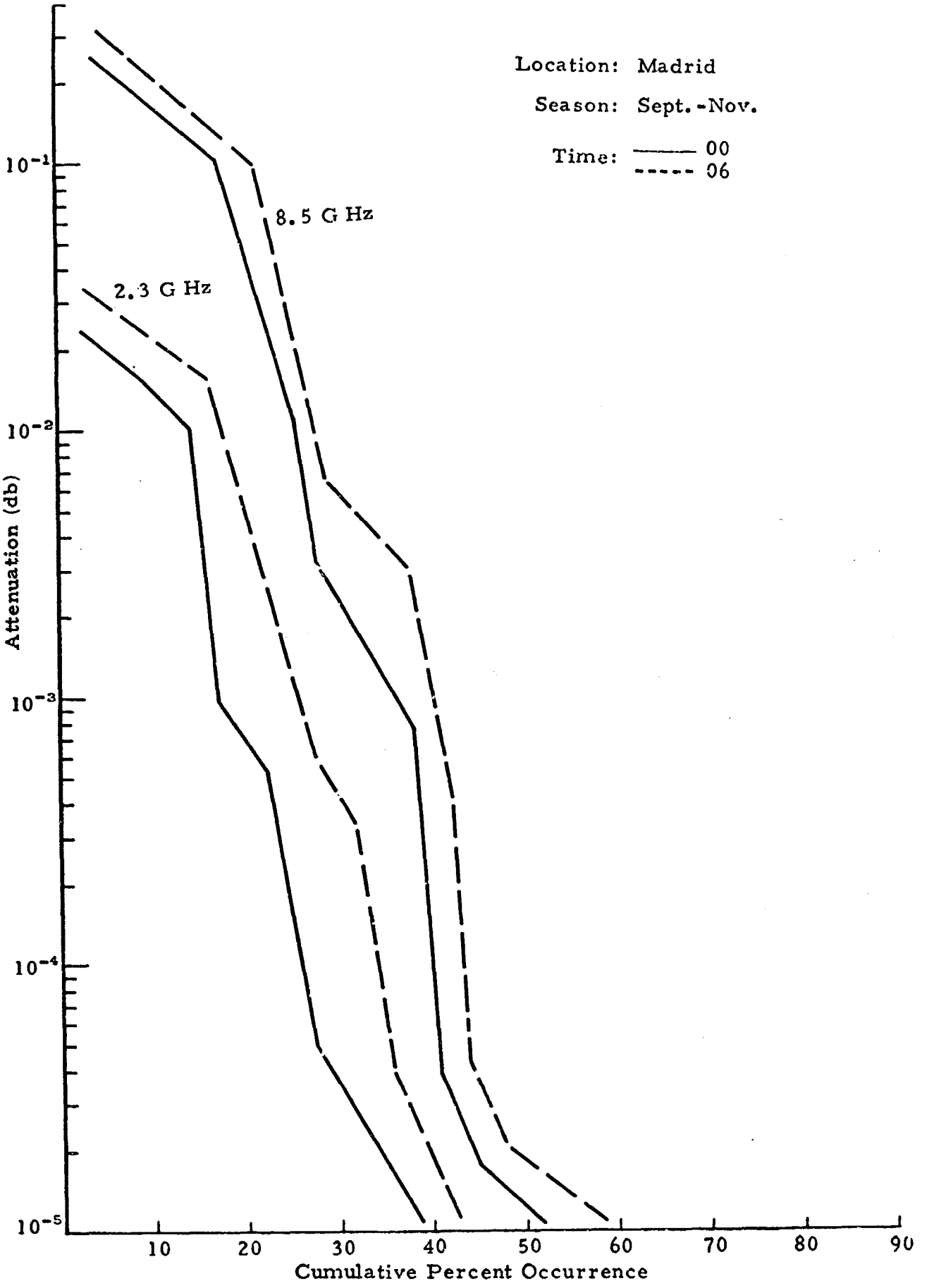

Fig. 20. ATTENUATION FACTORS

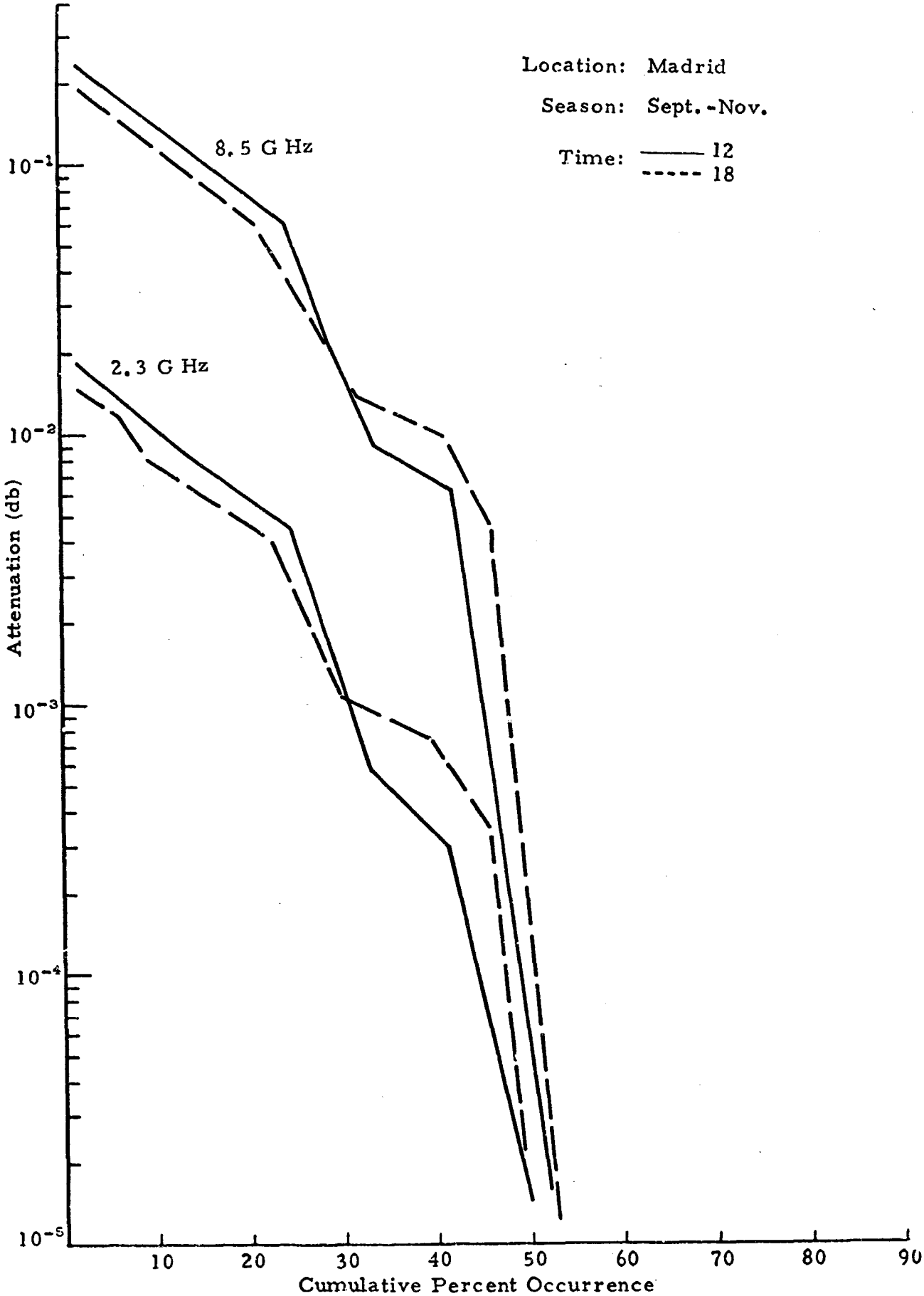

Fig. 21. ATTENUATION FACTORS

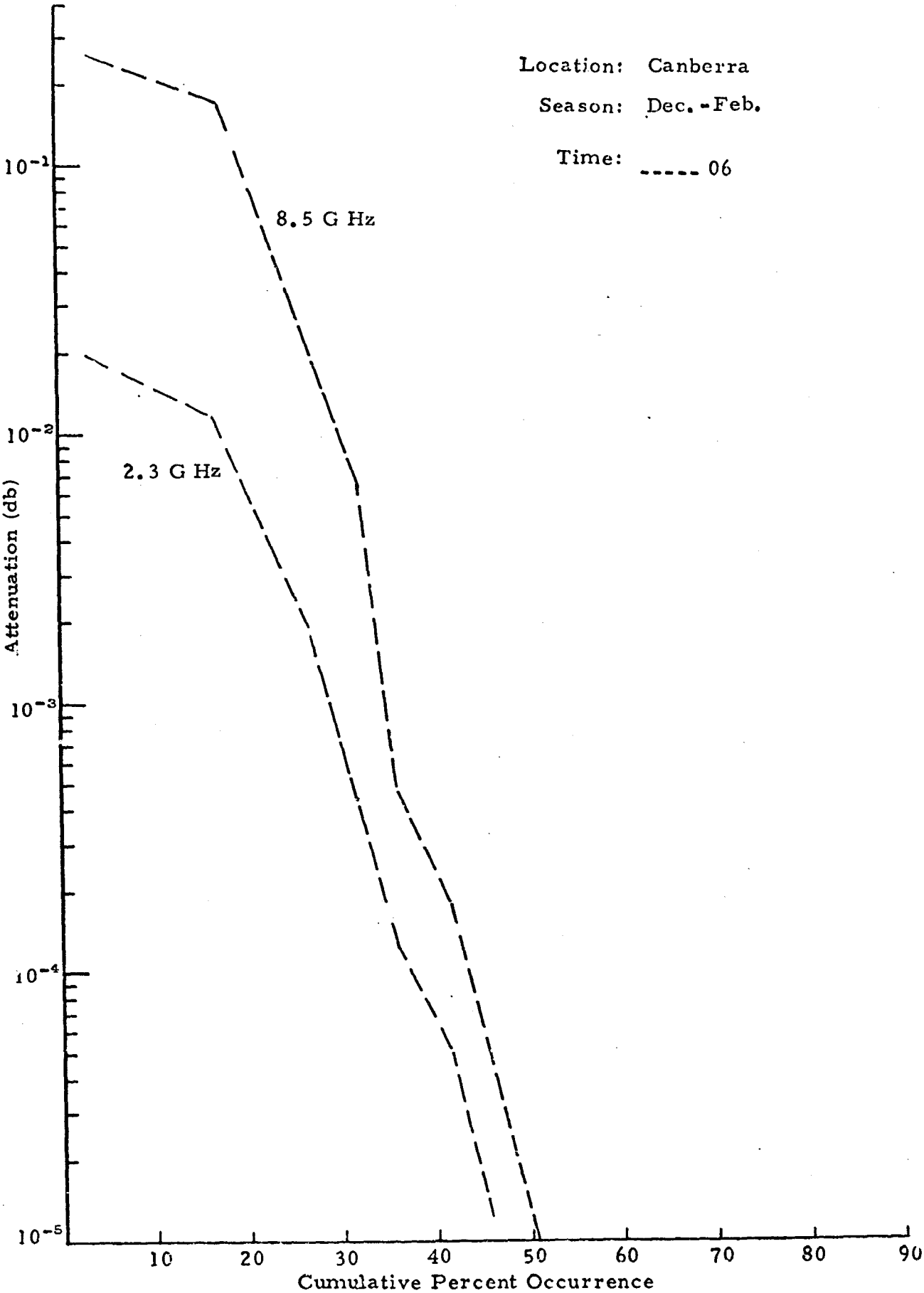

Fig. 22. ATTENUATION FACTORS

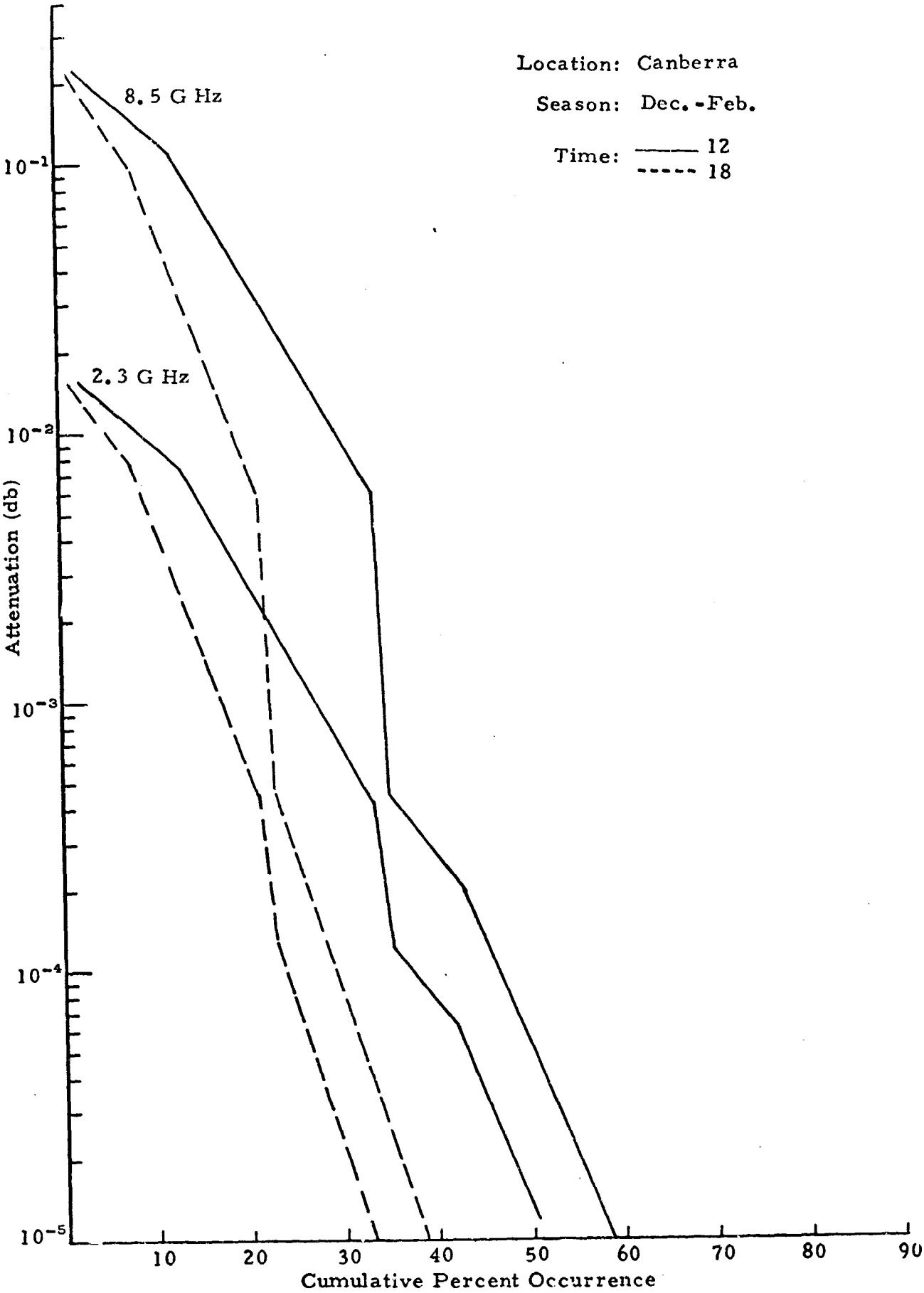

Fig. 23. ATTENUATION FACTORS

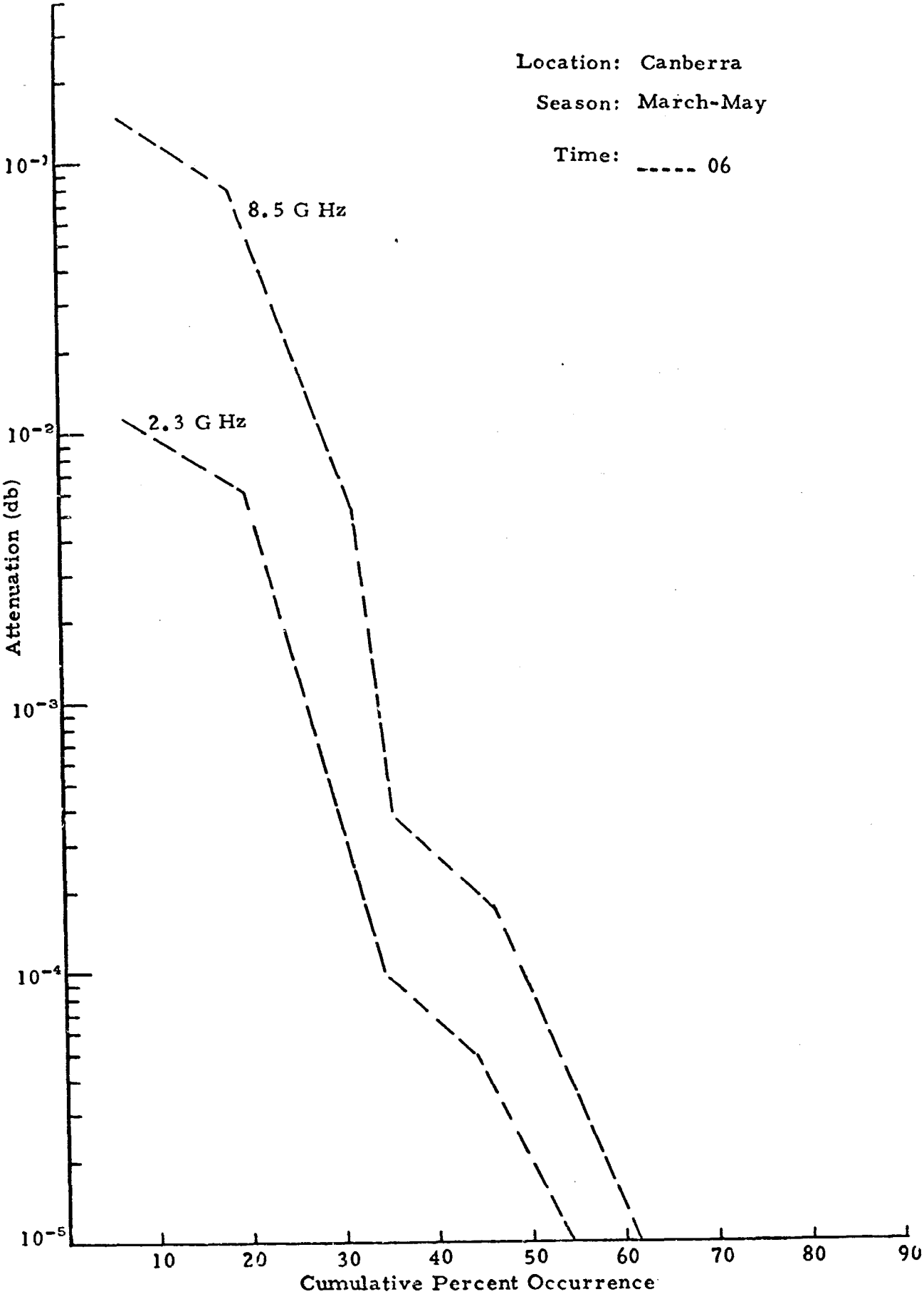

Fig. 24. ATTENUATION FACTORS

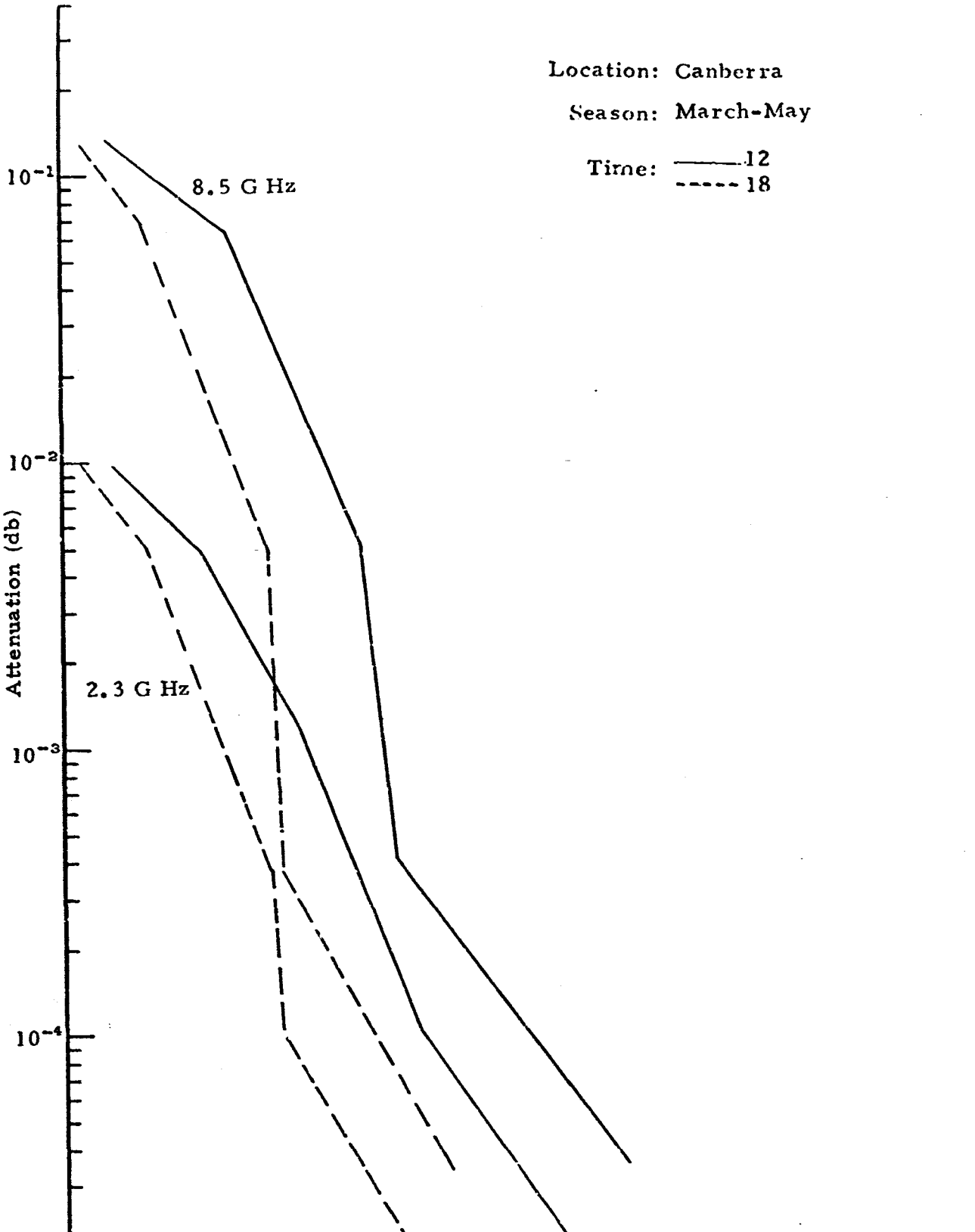

Fig. 25. ATTENUATION FACTORS

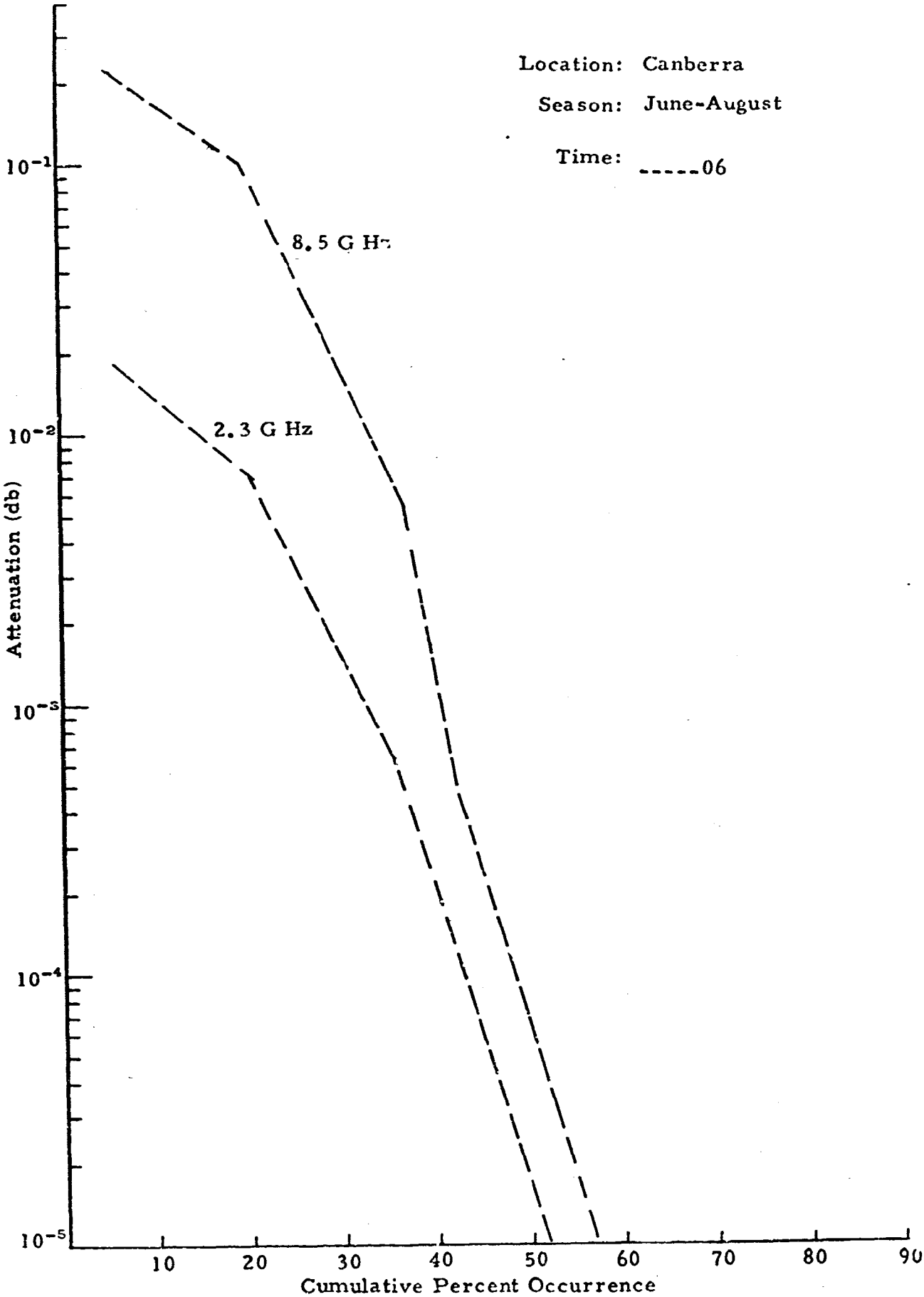

Fig. 26. ATTENUATION FACTORS

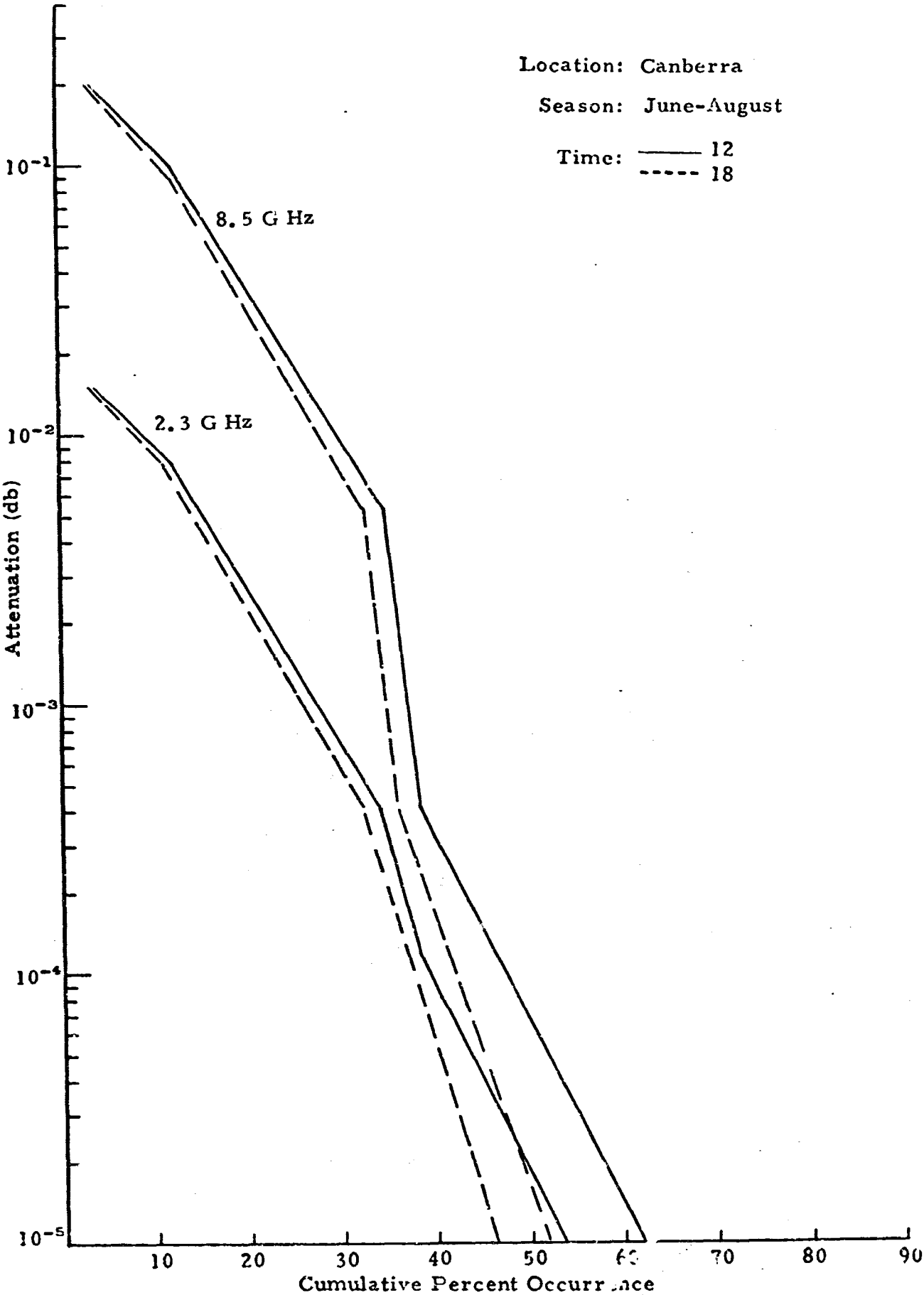

Fig. 27. ATTENUATION FACTORS

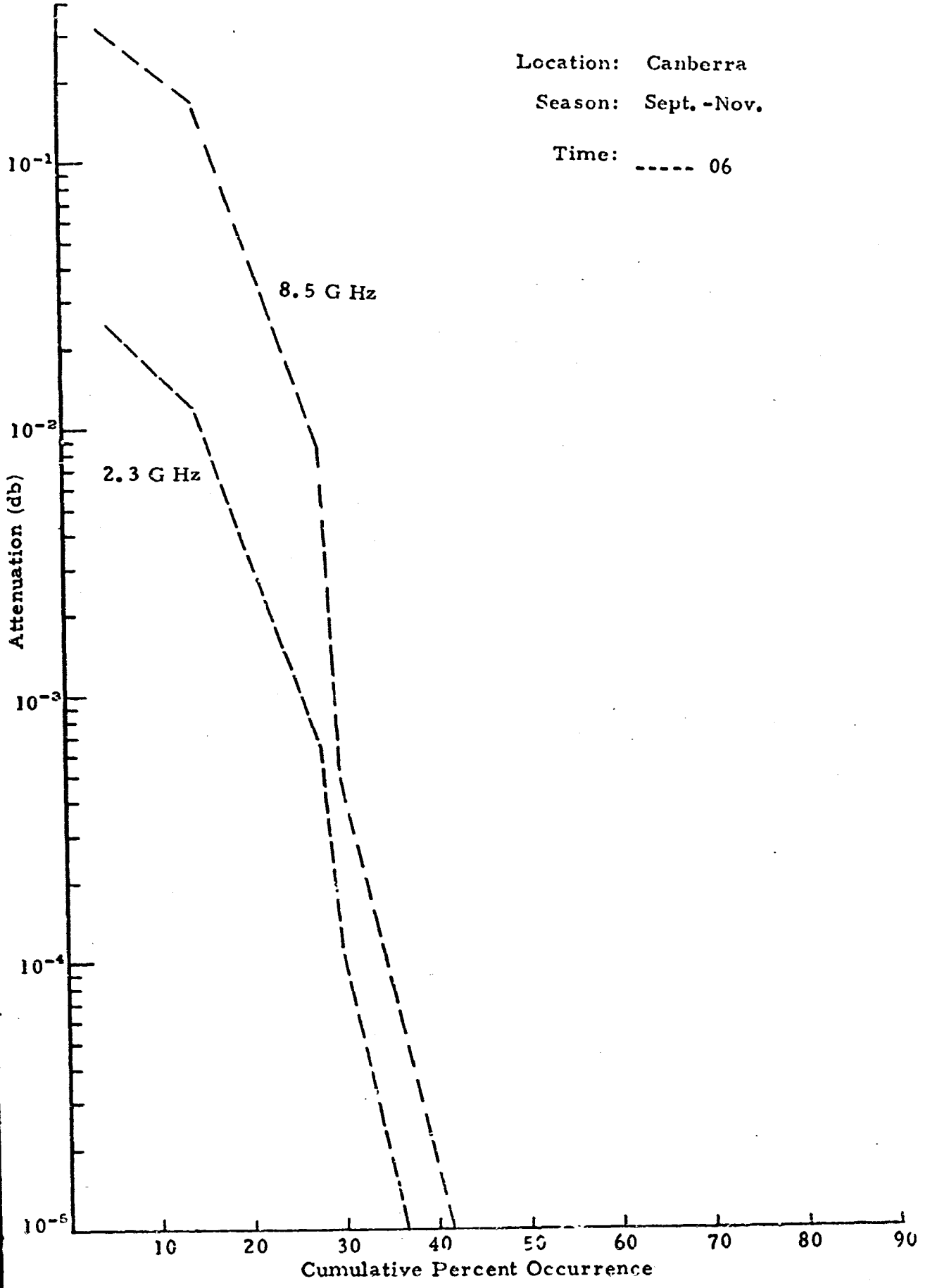

Fig. 28. ATTENUATION FACTORS

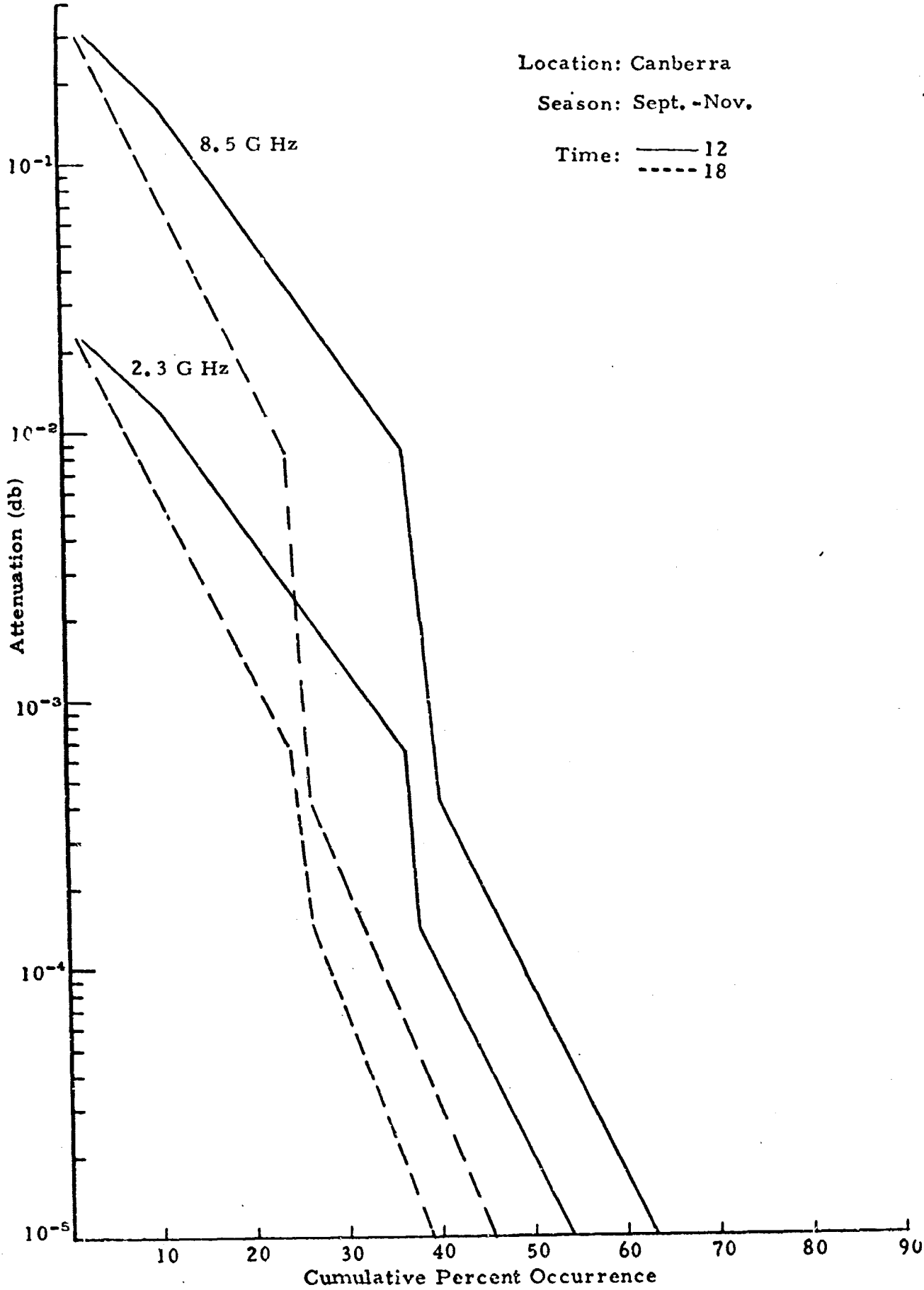

Fig. 29. ATTENUATION FACTORS

V. ERROR ANALYSIS

The nature of the attenuation calculations introduces several possible sources of error which deserve comment. These errors (or uncertainties) arise almost entirely from limitations in the observational data. Specific problems which arise in the calculations are described below together with estimates of the relative magnitude of the errors involved.

(a) Ice vs. Water - Description of the cloud droplets in terms of ice or water appears to be the major source of possible error in the attenuation calculations. A major difference exists between the index of refraction for small water and ice particles of the same size.

For the purposes of the present study, ice was assumed to occur at temperatures colder than -10°C with water drops at warmer temperatures. This places the low clouds at all sites in the water category. A computational discontinuity exists in the attenuation at the -10°C level which is neither realistic or definable within the observational data limitations. In reality, the transition from water to ice takes place over some considerable depth of cloud, particularly for cumulus clouds.

A change from water to ice at -10°C reduces the scattering coefficient (Q_s) by approximately a factor of four and the attenuation coefficient (Q_a) by a factor of 70-230. Fortunately, the total depth where some question of the presence of ice vs. water may arise is only a few thousand feet so that the error introduced in the total attenuation amounts to a factor of, perhaps, 10-25.

(b) Cloud Temperature - Variations in attenuation due to errors in temperature definition are negligible in comparison with the ice vs. water problem. For this reason, average temperatures were assumed for each cloud layer, low, middle, or high, for each computational day.

(c) Cloud Depth - Cloud depth enters the calculations in a linear manner. Data for Goldstone and Madrid were obtained from radiosonde observations which give moisture depths in the atmosphere each day. Clouds should be confined to these layers but might not fill the entire moisture depths. Errors of no more than a factor of two are likely from this source.

(d) Cloud Cover - Cloud cover also enters in a linear fashion. Cloud cover is observationally available and attenuation errors due to this cause should be less than a factor of two.

(e) Cloud Drop Characteristics - Cloud drop size enters into the calculation initially in the form ($\sim r^3$). Mean drop size is somewhat variable from one cloud type to another, from one day to the next, and the drop characteristics evolve with time during the lifetime of any given cloud. If the liquid water content of the cloud remains constant, changes in mean drop size of a factor of two would lead to errors of about eight in the attenuation calculation. If the liquid water also changes, as frequently happens in some portion of the cloud, the resulting error in computed attenuation would be larger. In the absence of observational data on time and space variations in drop sizes and number, constant values were assumed for the calculations.

(f) Time of Day - Goldstone and Madrid data show lowest attenuation values at 0000 local standard time. Characteristically, in most areas, cloud cover has a minimum during the nighttime hours. At Canberra, however, nocturnal low clouds form which lead to a relatively high cloud cover percentage at night or in the early morning.

The Goldstone and Madrid nocturnal data should be used with some caution. The minimum cloud cover at night is undoubtedly a real phenomenon in these areas but, traditionally, it is known to be exaggerated by the inability of observers to see cloud formations at night when they are actually present. This would apply particularly to high clouds and relatively thin clouds which produce low attenuation values anyway. Low clouds, particularly if overcast, are usually visible so that whatever error may exist in the attenuation statistics should apply principally to the low attenuation values.

(g) Rainfall - Attenuation calculations shown in the graphs assume no rainfall on any of the calculation days. In the event of rainfall, the attenuation would be substantially increased by the presence of large hydrometeors. Although actual observational data are not readily available, it is estimated that rain occurs at the various sites in approximately the manner shown:

Site	% of Hours with Rain
Goldstone	1
Madrid	8
Canberra	13

The rainfall, when it occurs, would fall on those days with greatest cloudiness and largest calculated attenuation. The table above indicates that the attenuation values on approximately 1-13 percent of the days (measured from the left-hand side of each chart) would be subject to higher values due to the presence of rain. Further refinement of these values could be made according to season but it was only intended here to indicate the general order of magnitude of the problem, i.e., that 1-13 percent of the hours would have larger attenuation values than shown in the graphs.

VI. CONCLUSIONS

Calculations of attenuation at 2.3 G Hz and 8.5 G Hz show expected variations at the three DSN sites: Goldstone, Madrid, and Canberra. In general, attenuation values are lowest at Goldstone and highest at Madrid. Highest values generally occur during the winter months and lowest (from a frequency of occurrence standpoint) during the summer. At Goldstone and Madrid, highest attenuation values occur during the noon or afternoon hours, lowest values are at night. Low clouds at Canberra during the night tend to make the attenuation values at 0600 local standard time relatively large.

Values of the attenuation calculated during the study are in general agreement with two other sources of information (Dutton, 1968, and Haroules and Brown, 1969). Somewhat different meteorological input parameters were used in the present study which has resulted, for example, in somewhat lower values than given by Dutton.

Principal errors in the calculations have been indicated to be (1) the difficulty in describing the constituency of the cloud in terms of ice or water for a range of cloud temperatures between, say, 0° to -15°C, and (2) the difficulty in defining drop size distributions (number and size) and their possible spatial and temporal variations. Possible errors in the computations suggest that the values should be correct within a factor of 10-20 on a statistical basis.

REFERENCES

Atlas, D., M. Kerker, and W. Hitschfeld, 1953: Scattering and attenuation by non-spherical atmospheric particles. J. Atmos. Terr. Phys., 3, 108-119.

_____, 1964: Advance in radar meteorology. Advances in Geophysics, 10, 318-468, Academic Press.

Battan, L. J., 1959: Radar Meteorology. University of Chicago Press, Chicago, Ill., 161 pp.

_____, and B. M. Herman, 1962: The radar cross section of "spongy" ice spheres. J. Geophys. Res., 67, 5139-5145.

Bean, B. R., and E. J. Dutton, 1966: Radio Meteorology. National Bureau of Standards Monograph 92.

Best, A. C., 1950: The size distribution of raindrops. Quart. J. Roy. Meteor. Soc., 76, 16-36.

Blanchard, D. C., 1953: Raindrop size distribution in Hawaiian rains. J. Meteor., 10, 457-473.

Dutton, E. J., 1968: Radio climatology for precipitation and clouds in central Europe. ESSA Research Laboratories, ERL 68-WPL 3.

Fletcher, N. H., 1962: The Physics of Rain Clouds. Cambridge Univ. Press, Cambridge, 386 pp.

Goldstein, L., 1946: Radio wave propagation experiments. Summary Tech. Rept., Commit. Propagation NDRC, 2, Washington.

Gunn, K. L. S., and T. W. R. East, 1954: The microwave properties of precipitation particles. Quart. J. Roy. Meteor. Soc., 80, 522-545.

Haroules, G. G., and W. E. Brown III, 1969: The simultaneous investigation of attenuation and emission by the earth's atmosphere at wavelengths from 4 centimeters to 8 millimeters. J. Geophys. Res., 74, 4453-4471.

Herman, B. M., and L. J. Battan, 1961: Calculation of Mie backscattering of microwave from ice spheres. Quart. J. Roy. Meteor. Soc., 87, 223-230.

_____, S. R. Browning, and L. J. Battan, 1961: Tables of the radar cross sections of water spheres. Arizona University Institute of Atmospheric Physics, Tech. Rept. 9.

Kerr, D. E. (ed.), 1951: Propagation of short radio wave. MIT Radiation Laboratory, Series 13, McGraw Hill.

Laws, J. O., and D. A. Parson, 1943: The relation of raindrop size to intensity. Trans. Amer. Geophys. Union, 24, 452-460.

Marshall, J. S., and W. M. K. Palmer, 1948: The distribution of raindrops with size. J. Meteor., 5, 165-166.

Mason, B. J., 1957: The Physics of Clouds. New York, Oxford Univ. Press, 481 pp.

Mie, G., 1908: Berträge zur Optik trüber Medien, speziell holloidaler Metallösungen. Ann. Phys., 25, 377-445.

Straton, J. A., 1941: Electromagnetic Theory. McGraw Hill.